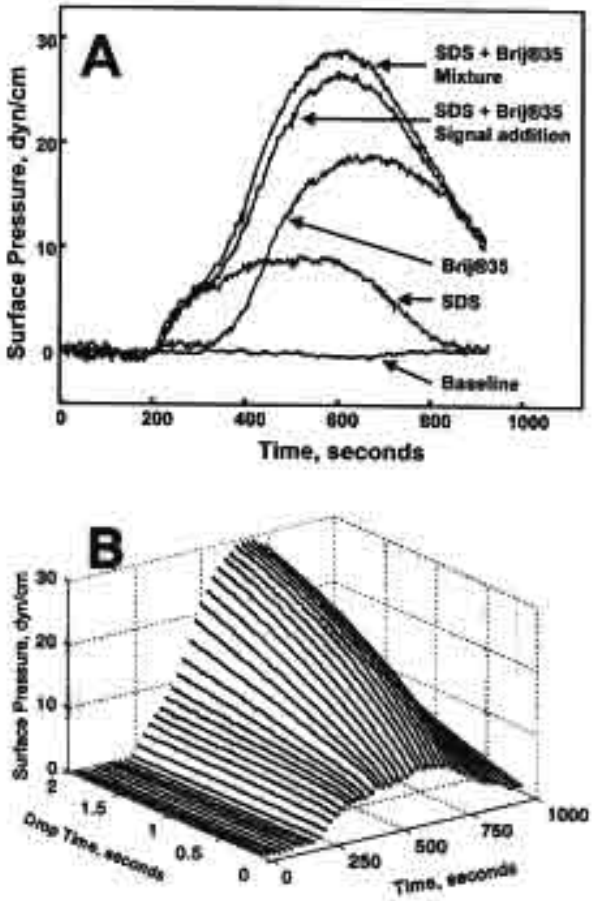

Fig. 3. The dynamic surface pressure plots of a 400 μl, 200 ppm Brij®35 concentration gradient mixed with a 500 μl, 2.0 mM SDS injection plug. (A) The overlay plots of the SIA plots for the average surface pressure at 1.8–2.0 s in the drop profile: baseline—dynamic surface pressure of water as baseline signal; SDS—dynamic surface pressure of SDS injection; Brij®35—dynamic surface pressure of Brij®35 gradient; SDS+Brij®35 mixture—dynamic surface pressure of SDS injection blended on-line with Brij®35 gradient; and SDS+Brij®35 signal addition—dynamic surface pressure of signal addition of individual SDS and Brij®35 signals. (B) Three-dimensional dynamic surface pressure plot of Brij®35 concentration gradient mixed with SDS injection. The drop time axis shows the surface pressure during the growth of individual drops (2 s each). For visual clarity only every tenth drop profile on the elution time axis was plotted.

sensor detects the surface activity of SDS only. In the third period, 320–600 s, the surface pressure plot shows the signal of the mixture, which consists of both the essentially steady-state concentration of SDS and the Brij®35 concentration gradient. In this region, various concentrations of Brij®35 are blended with the 2 mM SDS solution. In the last of the four time periods, 600–900 s, the surface pressure was returning back to baseline, indicating that the injection plug and gradient had both passed. With this particular mixture chemistry, the SDS and Brij®35 blend exhibits an additive effect of surface activity due to the presence of both analytes. That is, the signal of the SDS/Brij®35 mixture mimics that of the SDS signal added to the Brij®35 signal. This additive interaction has been observed in previous work [3] and is one type of interaction that is observed [14] in steady-state surface tension measurements. However, this surface tension interaction has never been observed with a high throughput system that measures multiple concentration combinations of two or more chemical components. The surface pressure at drop detachment of the mixture increased proportionately as the concentration of Brij®35 increased. By blending the steady-state concentration of 2 mM SDS as an injection plug zone with Brij®35, a concentration gradient zone in the concentration range 0–200 ppm is created. The kinetic surface pressure behavior of SDS mixed with various concentrations of Brij®35 is observed in Fig. 3B. The kinetic surface activity signal due to Brij®35 can be clearly delineated in the three-dimensional plot in Fig. 3B. The kinetic signal of Brij®35 becomes more pronounced when the concentration of Brij®35 in the mixture is increased. This behavior and the degree of interaction between SDS and Brij®35 can be explained from the compatibility of their molecular structures. SDS and Brij®35 both contain the same dodecyl hydrophobic chain. As the molecules align at the surface of the liquid–air interface, this hydrophobic region allows them to pack similarly alongside each other. In addition, the electrostatic repulsion forces between the anionic head groups of dodecyl sulfate at the drop liquid–air interface are minimized by the presence of the uncharged Brij®35 polar regions.

4.2. Kinetic surface pressure behavior of PEG 1470 with a Brij®35 concentration gradient

Using the same procedure and conception as the experiment of Brij®35 with SDS, the interfacial

properties of Brij®35 with PEG 1470 were studied. The signal profile results of Brij®35 concentration gradient blending with the PEG 1470 steady-state plug zone are shown in Fig. 4A and B. In Fig. 4A, the overlay plots are shown of surface pressure signal of baseline water, 50 ppm PEG 1470 alone, 100 ppm Brij®35 alone, PEG 1470 blending with the Brij®35 concentration gradient, and the signal addition of the individual Brij®35 and PEG 1470 signals. In this experiment, during the Brij®35 gradient that occured during the 320–600 s time period, the surface tension at drop detachment shows a competition effect between Brij®35 and PEG 1470. The signal for the mixture follows that of PEG 1470 alone until the point in time where the Brij®35 signal alone exceeds the PEG 1470 signal alone. At this point, the mixture signal follows that of Brij®35. The competition effect can be explained by molecular structure [3], since both hydrophobic chain groups are derived from the same PEG. Thus, when Brij®35 is mixed with PEG 1470 together in the system, the hydrophobic chain of Brij®35 (lauryl group) orients at the surface of drops. The kinetic surface pressure behavior of the mixture is shown in the three-dimensional plot in Fig. 4B. The increase in surface pressure during each growing drop shows the kinetic behavior of Brij®35 due to the dilation rate of the drop surface area being faster than the transportation rate of the Brij®35 molecule from the bulk solution to the surface of the drop. The kinetic surface pressure behavior effect of Brij®35 can be further evaluated by raising the concentration of Brij®35. These results are not shown for brevity.

4.3. Kinetic surface pressure behavior of SDS with TBA concentration gradient

The surface pressure plot results from the interfacial properties' study of SDS and TBA solutions are shown in Fig. 5A and B. A 400 μl, 1.0 mM TBA solution was delivered into the system to make the concentration gradient, and 500 μl of 1.0 mM SDS was injected to blend with TBA concentration gradient zone. By blending the two zones, the high throughput experiment region of various concentrations of TBA in 1.0 mM SDS was achieved. TBA alone is essentially non-surface active, as shown in Fig. 5A, and the counter-ion of TBA is hydroxide. SDS is an anionic surfactant, with the dodecyl sulfate (DS) acting as anionic group. When the TBA solution is mixed with the SDS solution in the system, DS and TBA can exhibit a kinetic surface pressure behavior, since

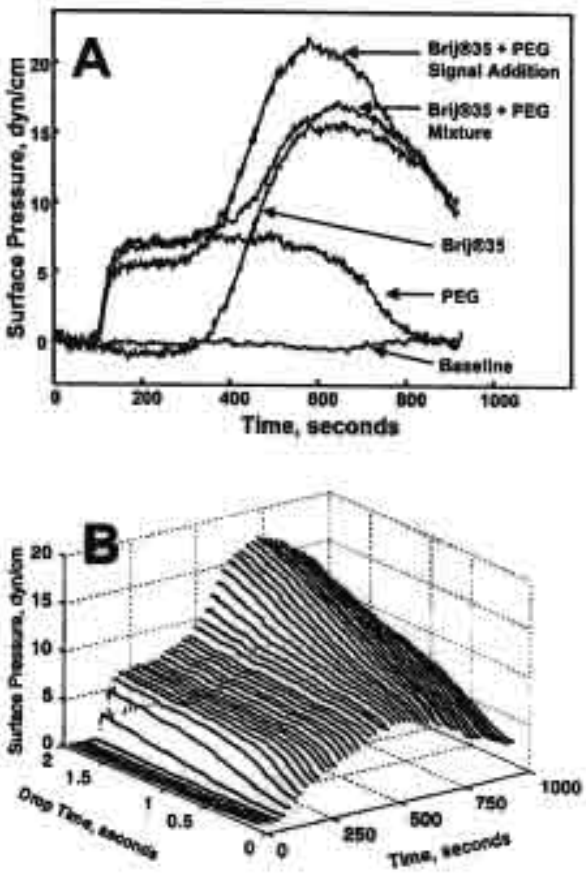

Fig. 4. The dynamic surface pressure plots of a 400 μl, 100 ppm Brij®35 concentration gradient mixed with a 500 μl, 50 ppm PEG 1470 injection plug. (A) The overlay plots of the SIA plots for the average surface pressure at 1.8–2.0 s in the drop profile: baseline—dynamic surface pressure of water baseline signal; PEG—dynamic surface pressure of PEG 1470 injection; Brij®35—dynamic surface pressure of Brij®35 gradient; PEG+Brij®35 mixture—dynamic surface pressure of PEG 1470 injection blended on-line with Brij®35 gradient; and PEG+Brij®35 signal addition—dynamic surface pressure of signal addition of individual PEG and Brij®35 signals. (B) Three-dimensional dynamic surface pressure plot of Brij®35 concentration gradient mixed with PEG 1470 injection. For visual clarity only every tenth drop profile on the elution time axis was plotted.

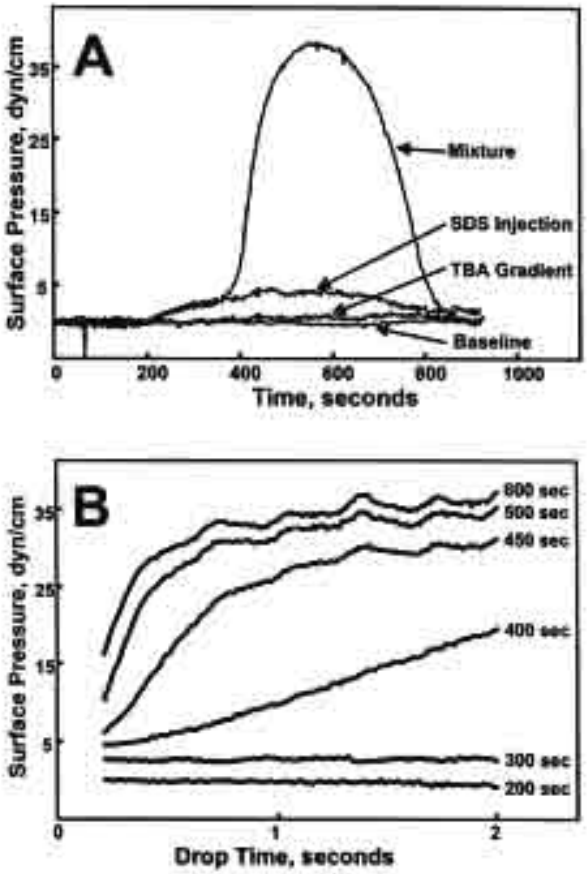

Fig. 5. Dynamic surface pressure plots of a 200 μl, 2.0 mM TBA concentration gradient mixed with a 500 μl, 1.0 mM SDS injection plug. (A) The overlay plots of the SIA plots for the average surface pressure at 1.8–2.0 s in the drop profile: baseline—dynamic surface pressure of water as baseline signal; TBA gradient—dynamic surface pressure of TBA gradient; SDS injection—dynamic surface pressure of SDS injection; and mixture—dynamic surface pressure of SDS injection mixed with TBA gradient. (B) Dynamic surface pressure plots for various elution times of SDS injection mixed with TBA gradient shown in (A), for elution times at 200, 300, 400, 450, 500, and 600 s.

an ion-pair of DS can form with TBA, similar to the other coordination surfactant systems. The enhancement of the surface activity of SDS by TBA was shown, in the time period between 350 and 600 s, in Fig. 5A. As the TBA concentration increases in 1.0 mM SDS solution, the surface pressure of each drop increases considerably. The change in the signal as the TBA concentration increases is shown in Fig. 5B. The SDS alone does not show the kinetic signal. The mixture of SDS and TBA does give a kinetic signal. The kinetic signal of the mixture is seen in the time window as the DSTD drop grows because of the higher packing of surfactant, DS, with TBA at the surface. Higher packing of SDS when TBA is present is indicated by the increase in surface pressure at drop detachment. Because the equilibrium surface concentration is higher when TBA is present, it takes longer to reach the equilibrium surface pressure [5]. The enhancement effect can be increased when the concentration of TBA is increased with time, as shown in both Fig. 5A and B.

4.4. Kinetic surface pressure behavior of SDS with a β-CD concentration gradient

Fig. 6 illustrates the surface pressure profiles of SDS alone, an on-line blending of SDS with a concentration gradient of β-CD, and the refractive index response of the β-CD concentration gradient alone. Since β-CD has no surface activity, DSTD was replaced with the refractive index detector to record the changes in β-CD concentration. The SDS profile shows the 500 μl, 3 mM SDS injection plug zone, and the β-CD profile shows the concentration gradient of 400 μl, 3 mM β-CD. When SDS and β-CD were mixed together in the system, it was shown that the surface pressure of the mixture decreases with an increase in β-CD concentration. This demonstrates that β-CD and SDS form an inclusion complex, and the inclusion complex does not respond to DSTD. When β-CD was present with SDS, the inclusion complex formed remains in the bulk drop solution. Thus, some fraction of the surfactant was essentially removed from the liquid–air interface. As seen in Fig. 6, as the β-CD concentration increases, the larger is the decrease in the surface activity of SDS present in the bulk solution. The surfactant/β-CD inclusion complex has been described in previous work [15–21]. It is well known that β-CD easily complexes with dodecyl sulfate, binding with a 1:1 mole ratio. β-CD is a cyclic oligosaccharide consisting of seven glucose units, and has a lipophilic cavity. When the surfactant binds with β-CD, methylene groups of a fully extended

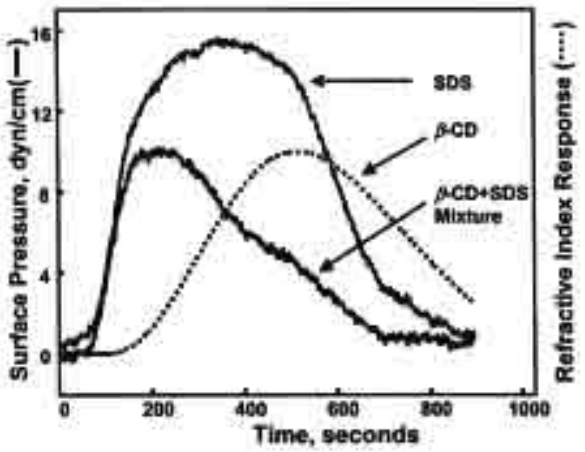

Fig. 6. The surface pressure overlay plots of a 400 μl, 3.0 mM β-CD concentration gradient mixed with a 500 μl, 3.0 mM SDS injection plug. The surface pressure signal from DSTD is shown as a solid line and the refractive index response from a refractive index detector is shown as a dashed line. The overlay plots of the DSTD data are for the average surface pressure at 1.8–2.0 s in the drop profile: SDS—surface pressure of SDS injection; β-CD—refractive index response of β-CD gradient; and β-CD + SDS mixture—surface pressure of SDS injection mixed with β-CD gradient.

hydrocarbon chain of surfactant are included in the cavity [19], thus, masking its surface hydrophobic character from exhibiting surfactant properties. From data, as shown in Fig. 6, one can readily extract the binding constant for the chemistry involved. In this case, the binding constant with dodecyl sulfate and β-CD was determined to be approximately 2500 M^{-1}. This method can be used in a general way to do drug binding studies with analytes such as proteins. Studies such as these are underway in our laboratory.

5. Conclusions

The study of interfacial properties of SDS in a Brij®35 gradient, PEG 1470 in a Brij®35 gradient, SDS in a TBA gradient, and SDS in a β-CD gradient was demonstrated experimentally with SIA/DSTD. An addition effect was observed with the SDS sample and a Brij®35 reagent gradient. A competition effect was observed with a PEG 1470 sample and a Brij®35 reagent gradient. An enhancement effect was observed with an SDS sample combined with a TBA reagent gradient. Finally, a bulk phase binding effect was observed with an SDS sample and a β-CD reagent gradient. SIA/DSTD introduces a high throughput, fast analysis method that does not require individual injections for each concentration of mixture samples. In this system, only a single concentration of sample and reagent was used to study the effect of sample in different concentrations of reagent. Thus, it consumed less reagent, produced less waste, and required significantly less analysis time than traditional FIA/DSTD.

Acknowledgements

We thank the Center for Process Analytical Chemistry (CPAC), the Thailand Research Fund (TRF), and the Royal Golden Jubilee Project (RGJ) for financial support.

References

[1] N.A. Olson, R.E. Synovec, W.A. Bond, D.M. Alloway, K.J. Skogerboe, Anal. Chem. 69 (1997) 3496.
[2] N.A. Olson, K.J. Skogerboe, R.E. Synovec, J. Chromatogr. A 806 (1998) 239.
[3] K.E. Miller, K.J. Skogerboe, R.E. Synovec, Talanta 50 (1999) 1045.
[4] K.E. Miller, R.E. Synovec, Anal. Chim. Acta 412 (2000) 149.
[5] W.W.C. Quigley, A. Nabi, B.J. Prazen, N. Lenghor, K. Grudpan, R.E. Synovec, Talanta 55 (2001) 551.
[6] M. Mulqueen, S.S. Datwani, K.J. Stebe, D. Blankschtein, Langmuir 17 (2001) 7494.
[7] M. Mulqueen, S.S. Datwani, K.J. Stebe, D. Blankschtein, Langmuir 17 (2001) 5196.
[8] B.M. Folmer, B. Kronberg, Langmuir 16 (2000) 5987.
[9] O.S. Sudah, G. Chen, Y.C. Chiew, Colloids Surf. B 13 (1999) 195.
[10] V.B. Fainerman, R. Miller, Colloids Surf. A 97 (1995) 65.
[11] S. Xu, S. Damodaran, Langmuir 10 (1994) 472.
[12] I.P. Purcell, J.R. Lu, R.K. Thomas, Langmuir 14 (1998) 1637.
[13] E. Alvarez, G. Vazquez, M. Sanchez-Vilas, B. Sanjurjo, J.M. Navaza, J. Chem. Eng. Data 42 (1997) 957.
[14] K. Tsujii, Surface Activity: Principle, Phenomena and Applications, Academic Press, San Diego, 1998, p. 245.
[15] T. Cserháti, J. Szejtli, Carbohydr. Res. 224 (1992) 165.

[16] Y. Saito, M. Abe, T. Sato, J.F. Scamehorn, S.D. Christian, Colloids Surf. A 119 (1996) 149.
[17] L.-R. Lin, Y.-B. Jiang, X.-Z. Du, X.-Z. Huang, G.-Z. Chen, Chem. Phys. Lett. 266 (1997) 358.
[18] R. Lu, J. Hao, H. Wang, L. Tong, J. Colloid. Interface Sci. 192 (1997) 37.
[19] X.-Z. Du, Y.-B. Jiang, L.-R. Lin, X.-Z. Huang, G.-Z. Chen, Chem. Phys. Lett. 268 (1997) 31.
[20] X.-Z. Du, Z. Yong, Y.-B. Jiang, L.-R. Lin, X.-Z. Huang, G.-Z. Chen, J. Photochem. Photobiol. A 112 (1998) 53.
[21] T.E. Young, K.E. Miller, R.E. Synovec, Microchem. J. 62 (1999) 70.

ผลงานวิจัย ก14

Available online at www.sciencedirect.com
SCIENCE DIRECT
Talanta 60 (2003) 1163–1170
Talanta
www.elsevier.com/locate/talanta

A simple flow injection-reduced volume column system for hemoglobin typing

Boonraksa Srisawang [a], Prachya Kongtawelert [b], Supaporn Kradtap Hartwell [a,*], Jaroon Jakmunee [a], Kate Grudpan [a]

[a] Department of Chemistry, Faculty of Science, Chiang Mai University, Chiang Mai 50200, Thailand
[b] Department of Biochemistry, Faculty of Medicine, Chiang Mai University, Chiang Mai 50200, Thailand

Received 12 September 2002; received in revised form 20 February 2003; accepted 5 March 2003

Abstract

A flow injection (FI)-reduced volume column system was developed for hemoglobin (Hb) typing to be used as an initial screening method for thalassemia. The column was packed with 140 μl diethylaminoethyl (DEAE)-Sephadex A-50 ion exchange beads. Hb can be separated using Tris–HCl buffer solution with pH gradient 8.5–6.5 and then monitored spectrophotometrically at 415 nm. The hemolysate of 40 blood samples from packed red cells were screened for thalassemia by determining the amount of HbA_2 and HbE present. The proposed system was able to predict positive test results from those samples with β, E-trait and EE homozygous thalassemia, Hb types that were independently identified following the conventional method at the hospital laboratory. Advantages of the proposed system over the conventional column technique include low amount of reagents and blood sample needed, short analysis time and low cost. Each analysis required only 80 μl of 50 times diluted packed cells, which is equivalent to 1.6 μl undiluted packed cells, and it can be completed in only 35 min. This simple FI-reduced volume column system was demonstrated to be an economic alternative system for Hb typing to initially screen some types of thalassemia such as β-trait, E-trait and EE-homozygous which are commonly found in Thailand.

Keywords: Flow injection; Hemoglobin typing; Reduced volume column

1. Introduction

Mutations of protein structure of the hemoglobin (Hb) are inherited through ancestor genes and cause many blood-related disorders such as Sickle Cell Anemia, and thalassemia. In Southeast Asia, Africa and Middle East, thalassemia trait is commonly found [1,2]. People with thalassemia trait are generally without health problems. However, if both parents have Hb variants (i.e. thalassemia trait), there is 25% chance that the baby will have homozygous variant (i.e. thalassemia disorder) [3].

Techniques commonly employed in the hospital to indicate the existence of thalassemia in patients are cellulose electrophoresis, micro-column chromatography and HPLC [4,5]. Electrophoresis can

* Corresponding author. Fax: +66-5-322-2268.
E-mail address: kradtas@yahoo.com (S.K. Hartwell).

0039-9140/03/$ - see front matter © 2003 Elsevier B.V. All rights reserved.
doi:10.1016/S0039-9140(03)00219-4

qualitate but cannot conveniently quantitate for different types of Hb. It is used to find out the exact type of thalassemia after the indication of having thalassemia was found. On the other hand, HPLC technique can be used to qualitatively and quantitatively analyze Hb but it requires an expensive instrumentation. Separation of Hb using DEAE-Sephadex column is well established and it is normally done to screen for thalassemia before performing further examinations. However, the conventional column technique involves analyzing many fractions of eluate collected batch-wise leading to long time, high amount of reagents and sample consumption. This work attempts to develop a simple, low cost and fast system to perform Hb typing.

In the proposed system, flow injection (FI) analysis coupled with a reduced volume chromatographic column for Hb separation has been developed. A flow based-system dramatically decreases the analysis time and can be automated [6,7]. Its closed system also reduces the possibility of sample contamination [8,9]. Hb typing is achieved using a reduced volume micro-DEAE-Sephadex ion exchange column that requires very small volume of diluted blood, which in turn generates only small amount of biological hazardous waste. The amount of Hb can be spectrophotometrically monitored at 415 nm. The technique is used to screen for some types of thalassemia based on abnormally high ratio of HbA_2 and HbE relatively compared with total amount of Hb as percentage. Comparison of the results with those obtained from the larger conventional column technique, indicates the possibility of applying the proposed system to initially screen for some types of thalassemia such as β-trait, E-trait and EE-homozygous before further conducting more expensive and conclusive testing.

2. Experimental

2.1. Combination of methods for thalassemia diagnosis

In regions where routine thalassemia testing is most needed due to its prevalence in the populations, such as in Southeast Asia and Africa, it is often also the case that economic restrictions on the medical systems prevent the use of the latest technologies that exist. In the laboratories that are not well equipped with more technically complicated instrumentation such as HPLC, diagnosis of Hb type is normally accomplished by conducting several different tests in combination, namely Osmotic Fragility Test (OFT), DEAE-column separation, HbE screening test (E-screen) and Polymerase Chain Reaction (PCR). OFT is a preliminary test based on the slower rupture rate of red blood cells of patients with thalassemia (positive) in hypotonic salt solution as compared with normal red blood cells (negative). DEAE-column separation can estimate percentage of HbA_2+HbE (positive when higher than 3.5%). E-screen is similar to the DEAE-column technique but the working buffer has precise pH that is more specific for HbE separation. Normal blood has less than 10% HbE (negative). Blood samples that have 25–30% HbE are considered as having HbE trait (positive) while those that have 70–90% HbE are identified as EE homozygous (positive). PCR-fluorescence spectrophotometry is used to indicate α-thalassemia gene in the patients who have normal level of HbA_2 with negative E-screen test. The relationship between results of each test and the diagnosis of Hb type is summarized as shown in Table 1.

2.2. Materials and apparatus

All pump tubings were tygon tubings (Saint-Gobain Performance Plastics, USA). The rest of the flow lines were assembled from PTFE tubings (Cole Parmer, USA). A peristaltic pump (FIA-lab, USA) was used to deliver buffer solutions. A reduced volume micro-column was made of acrylic piece into the dimension of 3 mm i.d. and 2 cm long. This dimension is much smaller than conventional column, which is about 1 cm i.d. and 5 cm long. It was packed with 140 μl of 40–120 μm DEAE-Sephadex A-50 beads (Phamasia Biotech, Sweden) which was about 20 times less than the amount of beads needed for packing a larger conventional column. Both sides of the column were sealed with cotton wool. Samples were

Table 1
Summarization of test results with diagnosis of Hb type

OFT	HbA_2 (conventional micro column)	E-screen	PCR	Hb type
+	–	–	–	A_2 normal
+	+ (>3.5%)	–	–	β-trait
+	+ (>60%)	+ (70–90%)	–	EE homozygous
+	+ (>3.5%)	+ (25–30%)	–	E-trait
+	–	–	+	α

introduced by means of a six port injection valve with an 80 μl sample loop. The flow through cell (HELLMA, Germany) with 1 cm path length was placed in the Spectronic 21 (Spectronic Instrument, USA). The detection of Hb was done at 415 nm. The absorbance data were converted to voltage and recorded with a computer software (Metex Corp., USA) installed in a personal computer (Compaq Presario 425). These data were transferred and integrated with Microsoft Excel (Microsoft Corp., USA).

2.3. Reagents

Tris–HCl 0.05 M buffer solutions of different pH values were prepared by dissolving 6.057 g Tris (hydroxymethyl) aminomethane (UBS, USA) and 0.1 g KCN (Riedel-De Haen Ag Seelze-Hannover, Germany) in 1000 ml distilled water and adjusted to the desired pH of 8.5, 7.5 and 6.5 with HCl (Merck, Germany). These three different pH buffers were used to create the pH gradient between 8.5 and 6.5.

2.4. Samples

Total of 40 blood samples (packed cells) were obtained from the Thalassemia Research Laboratories, Maharaj Nakorn Chiang Mai Hospital, Chiang Mai University where all subjects were routinely checked up. Each blood sample was hemolysed and diluted 50 times with Tris buffer pH 8.5 prior to use. The result from each sample was compared with the diagnosis result by the routine procedures of the hospital laboratory. The analytical procedures were independently run.

2.5. Manifold and operation steps

The diagram of a simple manifold used is shown in Fig. 1. Buffer solution pH 8.5 was pumped through the unloaded column to condition the column at a flow rate of 0.8 ml min^{-1}. Blood sample (80 μl) was injected into the system through a six port injection valve (V2). After the first peak of co-eluted HbA_2 and HbE appeared, the pH 8.5 buffer solution was replaced with pH 7.5 buffer solution by switching the valve V1. In between the gradient of pH 8.5 and 7.5, the HbA was eluted. Via the valve V1 then the buffer solution was again changed to pH 6.5 to elute out HbF. As a precaution the valve V3 can be used to drive off any observed air bubbles before they can get into the column.

3. Results and discussion

3.1. Elution profiles of hemoglobin

DEAE-Sephadex bead has diethylaminoethyl ($-OCH_2CH_2N^+H(CH_2CH_3)_2$) functional group that interacts with anionic groups on Hb and thus can retain all types of Hb. Different types of Hb contain different amount of net negative charge and, therefore, can be separated with the pH gradient elution. Upon elution using the more acidic buffer, containing more HCl, Hb becomes less negative and thus anionic groups of Hb captured by DEAE-bead can be exchanged with Cl^-. The order of Hb eluted from a DEAE-Sephadex column is HbA_2 co-eluted with HbE, then HbA and finally HbF [10,11].

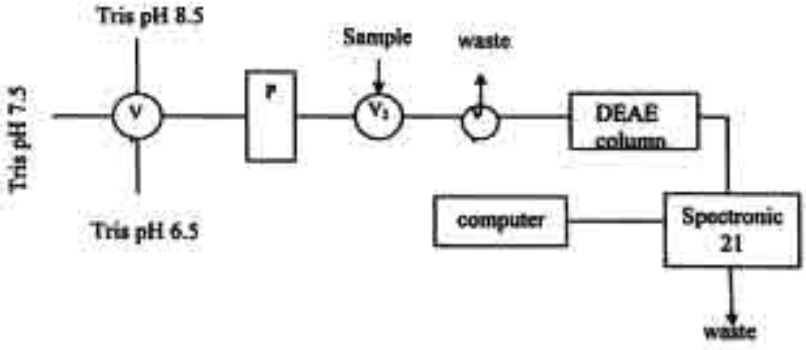

Fig. 1. Diagram of the simple FI manifold for Hb typing. V1, 4-ways valve; V2, six port injection valve; V3, 3-ways valve; P, peristaltic pump.

Examples of elution profiles of normal blood sample and that of EE-homozygous thalassemia patient obtained from the proposed system are illustrated in Fig. 2a and b, respectively. It should be noted that the *Y*-axis is in voltage that relates to transmittance and, therefore, peak height decreases with increasing of absorbance. The patterns of both elution profiles are similar but different in ratio of peak areas. Thalassemia patients have HbE that is coeluted with HbA_2 and, therefore, an abnormal blood sample shows larger first peak as compared with a normal blood sample.

3.2. Ratio of HbA_2 and HbE

Composition of Hb types in blood can vary depending on patient's age. Normal adult blood has been known to contain approximately 95–98% HbA, 2–3% HbA_2, and 0.8–2% HbF [12]. An individual with β-thalassemia trait usually has an elevated level of HbA_2, HbE and sometimes HbF along with the evidence of microcytosis and distinctive abnormal facial feature [2,4]. Patients with α-thalassemia, on the other hand, usually have HbA_2 and the same level as normal people have. Therefore, ratio of HbA_2 and HbE to total Hb cannot pinpoint what type of thalassemia the patient has without further examination.

From the elution profiles of blood samples, areas under each peak were integrated and the sum of those areas was counted as total Hb. The percentage of HbA_2+HbE was calculated from the ratio of area under HbA_2+HbE peak to the total area. Examples of calculation are also summarized in Fig. 2a and b. Even though ratio of HbA_2+HbE to total Hb cannot predict exactly what type of thalassemia the patient has, it can help indicate the existence of some types of thalassemia (i.e. β, EE homozygous, E trait types). The aim here is to utilize the benefits of the flow

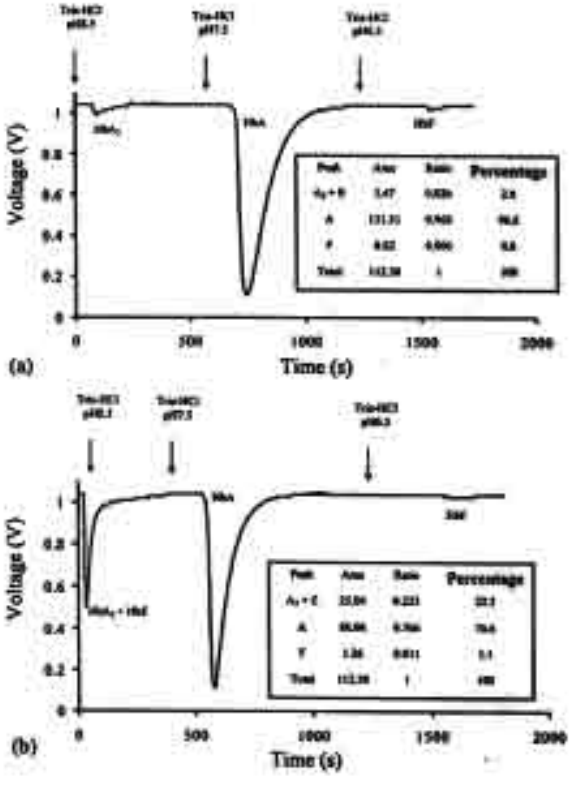

Fig. 2. FI-elution profiles of Hb in blood samples from (a) a normal adult and (b) an EE-homozygous thalassemia patient.

system combining with a DEAE-column technique and to show that the proposed FI-reduced volume column system can be used to initially screen for patients with some types of Thalassemia.

3.3. Evaluation of the proposed FI-system

In this work 40 adult blood samples (packed red cells) with positive OFT were examined without the prior knowledge of the type of Hb of each sample. Related to the hospital diagnostic results which were independently run, the correlation plot between the two systems, $R = 0.9271$, was obtained as shown in Fig. 3. The calculated percentages of HbA_2+HbE obtained from the proposed FI-reduced volume column system along with the results from a conventional column, E-screen and PCR are shown in Table 2(a) with a summary in Table 2(b). Two samples (one β-trait (18.4%) and one α-trait (17%)) were statistically eliminated from Table 2 because they gave results much higher than their standard ranges (β-trait 4–8%, α-thal-1-trait 2.5–3.5%) that are normally obtained using the HPLC. Because of the differences in the system characteristics and column size, the averages of HbA_2+HbE amounts obtained from different cases of thalassemia using the proposed system are lower than those obtained when using the conventional system, especially for the cases of E-trait and EE homozygous. The cause of deviation is currently under further investigation. However, the proposed system can differentiate normal and α-thal-trait samples (HbA_2+HbE < 3.5%) from abnormal samples (> 3.5%) and was still able to yield accurate positive test results. The level of HbA_2+HbE in EE homozygous samples was higher than in E-trait and β-trait samples, respectively, the same trends as indicated in the conventional column results.

For other types of Hb such as HbS, no testing could be conducted as there were no samples available in Thailand. However, according to a

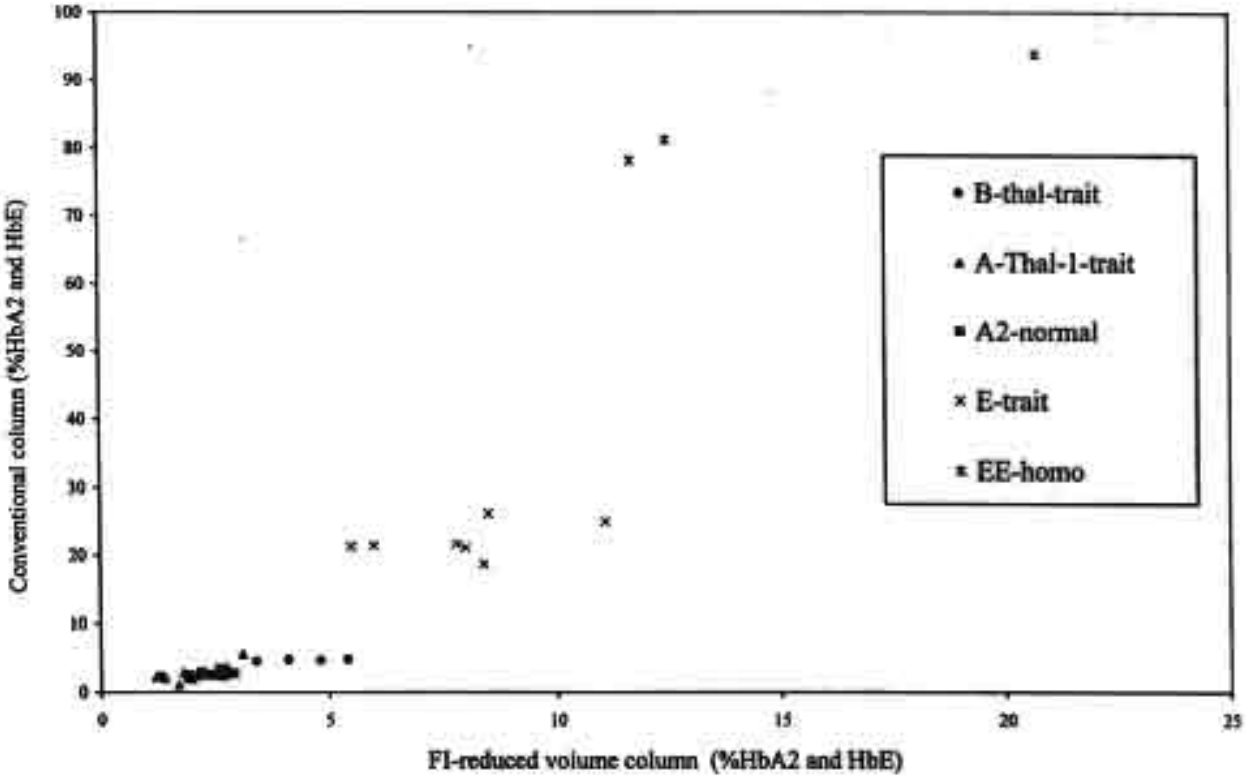

Fig. 3. Correlation plot between percentages of HbA_2+HbE obtained from the proposed FI-reduced volume column system and those obtained from the conventional column system.

Table 2
Comparison of calculated percentages of HbA_2 + HbE peak areas from the proposed FI-reduced volume column system* and from the conventional column system*

Sample	Percentages HbA_2 + HbE			E-screen*	PCR*	Hb type
	FI-red. V column*	Conventional column*	Ratio, FI-red. V: convention			
(a)						
A4	2.6	2.9	1:1.1	−	−	A_2-Normal
B6	1.3	2.2	1:1.7	−	−	A_2-Normal
B11	2.2	2.9	1:1.3	−	−	A_2-Normal
B13	1.9	2.5	1:1.3	−	−	A_2-Normal
B15	2.6	3.4	1:1.3	−	−	A_2-Normal
B16	2.7	3.4	1:1.3	−	−	A_2-Normal
C3	1.9	2.5	1:1.3	−	−	A_2-Normal
C25	2.8	2.8	1:1.0	−	−	A_2-Normal
D17	2	2.3	1:1.2	−	−	A_2-Normal
E6	2.6	2.4	1:0.9	−	−	A_2-Normal
E25	2.3	2.6	1:1.1	−	−	A_2-Normal
F18	2.4	2.5	1:1.0	−	−	A_2-Normal
C8	2.9	2.7	1:0.9	−	−	A_2-Normal
C5	3.4	4.5	1:1.3	−	−	β-Thal-trait
D3	5.4	4.8	1:0.9	−	−	β-Thal-trait
D9	4.1	4.7	1:1.1	−	−	β-Thal-trait
D18	7.3	18.4	1:2.5	−	−	β-Thal-trait
E24	4.8	4.6	1:1.0	−	−	β-Thal-trait
A9	1.8	2.9	1:1.6	−	+	α-Thal-1-trait
A8	3.1	5.5	1:1.8	−	+	α-Thal-1-trait
A28	2	2.5	1:1.3	−	+	α-Thal-1-trait
B2	2.2	2.5	1:1.1	−	+	α-Thal-1-trait
C2	1.7	1.1	1:0.6	−	+	α-Thal-1-trait
C11	1.4	2	1:1.4	−	+	α-Thal-1-trait
C12	1.2	2.2	1:1.8	−	+	α-Thal-1-trait
C16	2.7	2.4	1:0.9	−	+	α-Thal-1-trait
D2	1.3	2.2	1:1.7	−	+	α-Thal-1-trait
E7	1.9	2.1	1:1.1	−	+	α-Thal-1-trait
E10	2	1.9	1:1.0	−	+	α-Thal-1-trait
E20	8.5	17	1:2.0	−	+	α-Thal-1-trait
A1	5.5	21.3	1:3.9	+	−	E-trait
A23	8	21.1	1:2.6	+	−	E-trait
B4	8.4	18.7	1:2.2	+	−	E-trait
C13	6	21.4	1:3.6	+	−	E-trait
D20	11.1	25	1:2.3	+	−	E-trait
E19	8.5	26.1	1:3.1	+	−	E-trait
C7	7.8	21.7	1:2.8	+	−	E-trait
A39	12.5	81.2	1:6.5	+	−	EE-homo
C24	11.7	78.2	1:6.7	+	−	EE-homo
A37	20.7	93.8	1:4.5	+	−	EE-homo

Table 2 (*Continued*)

Hb type	HbA_2+HbE percentage				
	FI-reduced volume column*		Conventional larger column*		Standard range (HPLC)*
	Range	Average ± S.D.	Range	Average	
(*b*)					
A_2-normal (13)*	1.3–2.9	2.3 ± 0.1	2.2–3.4	2.7	2.5–3.5
α-thal-1-trait (11)*	1.2–3.1	1.8 ± 0.1	1.1–2.9	2.5	2.5–3.5
β-thal trait (4)*	3.4–5.4	4.1 ± 0.2	4.5–4.8	4.6	4.0–8.0
E-trait (7)*	5.5–11.1	8.0 ± 0.1	18.7–26.1	22.2	> 10
EE-homo (3)*	11.7–20.7	14.3 ± 0.9	78.2–93.8	84.5	> 60

(a) Results from each samples are shown along with the results from E-screen*, PCR-fluorescence spectrometry* and Hb Type diagnosis that were done by the Thalassemia Research Laboratories, Maharaj Nakorn Chiang Mai Hospital, Chiang Mai University (+ is positive result and − is negative result). (b) Summarization of ranges of HbA_2+HbE percentages and average values obtained when using the proposed and conventional column systems. *Independently run. Note: there were no S.D. data for the results obtained from the conventional column.

* Number of samples for each Hb type.

previous study by Dozy et al. [5], the DEAE column can separate Hb by descending pH gradient between 8.5 and 7.0. The order of Hb eluted from the column were HbA_2, HbS, HbA and finally HbF, respectively, in that study. Similarly, in this proposed study, HbA_2, HbA and HbF were eluted in the same order based on a similar pH range. Therefore, this proposed method should be able to screen for HbS if it is contained within the sample.

Reproducibility of the system was tested by running seven replicates of three samples (normal, β-trait and E-trait) each of which represented different levels of HbE. R.S.D. of the method was found to be 3.4% for normal sample and 4.6% for both β-trait and E-trait samples.

3.4. Advantages and disadvantages

The DEAE column technique has two main disadvantages. Neither the proposed nor the conventional column systems can point out patients with α-thalassemia due to non-differentiated level of HbA_2+HbE from normal people, in which case PCR result is needed. Also, both the proposed reduced volume column and the conventional column systems have another similar inconvenience in that they have to be repacked after each run due to constriction of the flow caused by coagulation of some matrices in blood. However, using a fresh column each time will eliminate the carry over effect from the previous run.

In the proposed FI-reduced volume column system, the improvement comes from the reduction in the amount of beads used and the time it takes for column packing, both of which are minimized as compared with those of the conventional column. The proposed system offers other advantages such as ease of operation, low cost, small amount of sample, and fast analysis time. The analysis time using the FI-reduced volume column is about 35 min per sample as compared with 4 h using a conventional column. Amount of sample for each run was as little as 80 μl of 50 times diluted sample, a major improvement as compared with the 2 ml of undiluted packed cell that is needed for a conventional column technique.

4. Conclusion

The FI-reduced volume column system for Hb typing was developed. The system was used as an initial screening for some types of thalassemia such

as β-thal-trait, E-trait and EE-homozygous which are commonly found in Thailand. It was demonstrated that the proposed system could differentiate normal blood samples from abnormal ones. Although the cause of deviation between results from the proposed system and those from the larger conventional column technique normally performed in the hospital needs further investigation, the proposed system was still able to predict positive test results. This preliminary study shows that the proposed system offers some advantages over the conventional column technique, including a simpler instrumentation with ease of operation, shorter analysis time and lower amounts of sample and reagents needed. These benefits will help reduce the overall analysis cost and should be useful as an economic alternative technique for routine thalassemia screening involving a large number of blood samples.

Acknowledgements

The Thailand Research Fund (TRF) is thanked for the financial support. Postgraduate Education and Research Program in Chemistry (PERCH) is acknowledged for partial support. The authors also thank Professor Torpong Sa-nguansermsri, Kullaya Payu and Rattika Saetung from Thalassemia Research Laboratories, Maharaj Nakorn Chiang Mai Hospital, Chiang Mai University for blood samples and comparison of diagnosis results.

References

[1] S. Fucharoen, Thalassemia, Regional Workshop on Abnormalities of Protein in Relation to Human Diseases, Chulabhorn Research Institute, Bangkok, Thailand, 1–5 September 1997, pp. 2.1–2.19.
[2] D.J. Weatherall, J.B. Clegg, The Thalassemia Syndromes, fourth ed., Blackwell Science, New York, 2001.
[3] C.K. Matthews, K.E. Van Holde, Biochemistry, second ed., Benjamin/Cummings, New York, 1992, pp. 214–257.
[4] T. Tata, P. Gategasem, P. Hathirat, Southeast Asian J. Trop. Med. Public Health 28 (2) (1997) 417.
[5] A.M. Dozy, E.F. Kleihauer, T.H.J. Huisman, J. Chromatogr. 32 (1968) 723.
[6] K. Grudpan, Lab. Robot. Autom. 12 (2000) 127.
[7] W. Kunawanakit, S. Jungkasemchokchai, N. Worakitcharoenchai, J. Jakmunee, K. Grudpan, Lab. Robot. Autom. 12 (2000) 164.
[8] Z. Fang, Flow Injection Atomic Absorption Spectroscopy, Wiley, New York, 1995.
[9] K. Grudpan, K. Kamfoo, J. Jakmunee, Talanta 49 (1999) 1023.
[10] T. Chamrasratanakorn, T. Sanguansermsri, A. Punyakeaw, Bull. Chiang Mai Assoc. Med. Sci. 31 (1998) 32.
[11] W. Bumrung, Hemoglobin Typing with Cation Exchange HPLC, B.S. thesis, Department of Medical Technology, Chiang Mai University, Chiang Mai, Thailand 1993.
[12] D. Voet, J.D. Voet, Biochemistry, second ed., Wiley, New York, 1995, p. 1142.

Available online at www.sciencedirect.com
SCIENCE DIRECT®
Analytica Chimica Acta 499 (2003) 191–197
ANALYTICA CHIMICA ACTA
www.elsevier.com/locate/aca

Flow injection analysis of tetracycline in pharmaceutical formulation with pulsed amperometric detection

Sanit Palaharn [a], Thiraporn Charoenraks [a], Nattakarn Wangfuengkanagul [a], Kate Grudpan [b], Orawon Chailapakul [a,*]

[a] Department of Chemistry, Faculty of Science, Chulalongkorn University, Bangkok 10330, Thailand
[b] Department of Chemistry, Faculty of Science, Chiang Mai University, Chiang Mai 50200, Thailand

Received 13 March 2003; received in revised form 14 July 2003; accepted 17 July 2003

Abstract

A flow injection method with pulsed amperometric detection (PAD) was proposed for the determination of tetracycline in pharmaceutical formulations. Tetracycline was also studied at a gold rotating disk electrode with cyclic voltammetry as a function of the pH of supporting electrolyte solution. The well-defined cyclic voltammogram, providing the highest peak current at 1.15 V versus Ag/AgCl, was obtained when using potassium dihydrogen phosphate solution at pH 2. The optimized pulsed amperometric detection conditions were 1150 mV (versus Ag/AgCl) detection potential (E_{det}) for 600 ms (500 ms delay time and 100 ms integration time), 1600 mV (versus Ag/AgCl) oxidation potential (E_{oxd}) for 150 ms oxidation time (t_{oxd}) and 100 mV (versus Ag/AgCl reference electrode) reduction potential (E_{red}) for 300 ms reactivation time (t_{red}). The optimized PAD waveform was applied to the determination of tetracycline standard solution and tetracycline in pharmaceutical formulations. The sensitivity of this method was found to be 13.7 μA/mM. The determination of tetracycline in commercially available tablet dosage forms by the proposed method (254.3 ± 9.3 mg per capsule) was comparable to those labeled (250 mg per capsule).

Keywords: Tetracycline; Gold electrode; Pulsed amperometric detection; Flow injection analysis

1. Introduction

Tetracycline is an antibiotic with a broad spectrum of activity against bacteria. It is used for many different infections, such as respiratory tract infections, urethritis and severe acne. It also has a role in the treatment of multidrug resistant malaria. Adverse effects include gastrointestinal disturbances, renal dysfunction, hepatotoxicity, raised intracranial pressure and skin infections, such as rosacea and perioral dermatitis. Various methods have been used for the determination of this compound. Spectrophotometric [1,2], fluorimetric [3–7], chemiluminometric [8–10], microbiological [11–13] and electrochemical [14–19] methods have been suggested. Electrochemical methods are of more interest than the others due to simplicity, less time analysis and low cost. Flow injection analysis can be applicable to electrochemical method, such as flow injection amperometric detection based on ion transfer across water-solidified nitrobenzene interface to determine tetracycline [18]. The results showed very low detection limit of 20 ng and the linear concentration range of 0.002–0.2 mM. Polarographic methods offer high sensitivity but their drawback is the use of mercury and they may not be practical for many applications, including flow injection. Although

* Corresponding author. Tel.: +66-2-218-7615; fax: +66-2-254-1309.
E-mail address: corawon@chula.ac.th (O. Chailapakul).

0003-2670/$ – see front matter © 2003 Elsevier B.V. All rights reserved.
doi:10.1016/S0003-2670(03)00948-6

voltammetry and amperometry also offer high sensitivities, their major disadvantage is deposition of the detection products and/or solution impurities on the electrode surface. Thus mechanical polishing is used to reactivate electrode surface and this is known to temporarily alter the response of a working electrode, often requiring 60–90 min before a stable baseline is obtained [20]. Therefore, pulsed amperometric detection (PAD) at a noble metal electrode which combines amperometric detection with alternated anodic and cathodic polarization to clean and reactivate the electrode surface, has been introduced to overcome this problem [21–24]. In contrast to simple amperometric detection, PAD offers the possibility to clean and regenerate the electrode surface effectively after each measuring cycle without the need for mechanical polishing. In the simplest implementation of PAD, the potential of the working electrode is stepped between the potentials for detection, E_{det}, cleaning, E_{oxd}, and reactivation, E_{red}. The cleaning and reactivating pulses maintain constant responsivity from injection to injection. All three variants of PAD require the following: (a) the analytes are oxidized during the detection step; (b) the oxidation products are removed from the electrode surface at E_{oxd}; (c) the oxide film, which inhibits the oxidation of analytes, is reduced at E_{red} [25]. Pulsed amperometric detection at gold or platinum electrodes has been used for the sensitive detection of numerous polar compounds [26–34] and metal species [35]. The difficulties resulting from electrode fouling are also avoided. To obtain fast and reproducible results, many reports also introduced flow injection analysis for the determination of tetracycline [36,37].

The goal of this work is optimization of the PAD waveform for the determination of tetracycline in pharmaceutical formulations. Furthermore, flow injection analysis, which provides fast, repetitive and reproducible analysis, has been combined with PAD to reduce the analysis time and to obtain a lower detection limit.

2. Experimental

2.1. Chemicals and reagents

All chemicals were analytical grade and all solutions were prepared by using deionized water. Phosphate solutions for (for pH 2, 2.5, 3, 3.5, 4, 4.5) were prepared from 0.1 M potassium dihydrogen phosphate (Merck) and adjusted to the desired pH using 85% phosphoric acid (J.T. Baker) solution in 0.1 M sodium hydroxide solution (for pH 5, 5.5, 6, 6.5, 7, 8, 9, 10). Standard tetracycline hydrochloride (Sigma–Aldrich) solutions were freshly prepared in 0.1 M potassium dihydrogen phosphate solution prior to use.

A stock solution containing 481 $\mu g\,ml^{-1}$ (1 mM) of tetracycline hydrochloride in 0.1 M potassium dihydrogen phosphate solution (pH 2) was used to prepare standards in four 10 ml volumetric flasks. The final concentrations of the standard solutions were 24.1, 48.1, 96.1, and 144.3 $\mu g\,ml^{-1}$, respectively.

All solutions were protected from exposure to light with aluminium foil and stored at <4 °C in an ice bath.

2.2. Sample preparation

Tetracycline hydrochloride capsules (250 mg TC-mycin, Vesgo, USA) were used in this study.

The powder from 10 capsules was dissolved in 0.1 M potassium dihydrogen phosphate solution (pH 2) in a 1000 ml volumetric flask, and then filtered through a 0.45 μM nylon membrane syringe filter. The filtrate was further diluted with 0.1 M potassium dihydrogen orthophosphate solution (pH 2) to obtain a final concentration of 0.2 mM (calculated from the label value). This sample preparation has been repeated for five times.

2.3. Electrode

The gold rotating disk electrode (Au RDE, Metrohm, Switzerland) and gold disk electrode (Bioanalytical System, West Lafayete IN, USA) were pretreated by polishing with 0.05 μm of alumina/water slurries on a felt pad, followed by rinsing with ultra pure water prior to use.

2.4. Rotating disk voltammetry

Electrochemical measurements were carried out in a single compartment three electrode glass cell. The rotation speed was held at 250 rpm. A Ag/AgCl electrode and a platinum electrode were used as

the reference and auxiliary electrodes, respectively. Cyclic voltammetry was performed with an Autolab Potentiostat 100 (Metrohm, Switzerland).

2.5. Flow injection analysis with pulsed amperometric detection

The flow injection analysis system consisted of a thin-layer flow-through electrochemical cell (Bioanalytical System, Inc.), an injector port (Rheodyne 7125) with a 20 μl sample loop, a peristaltic pump (BIO-RAD) and an electrochemical detector (PG 100). The carrier solution, 0.1 M potassium dihydrogen phosphate, was regulated at a flow rate of 1.0 ml min^{-1}. The thin-layer flow, through electrochemical cell consisted of a silicone rubber gasket as a spacer, a gold disk electrode as the working electrode, a Ag/AgCl electrode as the reference electrode and a stainless steel tube as the auxiliary electrode and the outlet from the flow cell. The experiments were performed in a Faraday cage to reduce the electrical noise. The PAD waveform used to obtain the FI–PAD response is depicted in Fig. 1.

The FI–PAD response was monitored for independent variation of all potential and time parameters. The electrode was conditioned in a solution of 0.1 M potassium dihydrogen phosphate solution and pumped through the flow system at a constant flow rate of 1.0 ml min^{-1} with the selected PAD waveform until a stable baseline was established. The sample was then injected into the flow injection system via an injection valve equipped with a fixed sample loop of 20 μl and the resulting peaks were recorded.

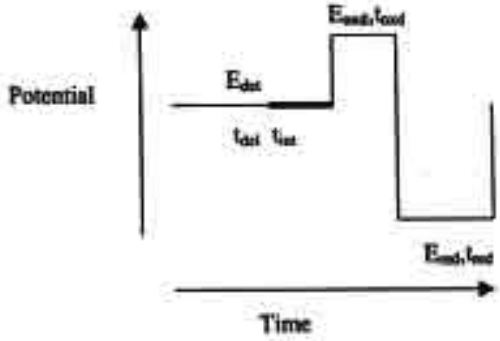

Fig. 1. Typical PAD waveform.

3. Results and discussion

3.1. pH dependence study

The electrochemical behavior of tetracycline was studied at the Au RDE in 0.1 M potassium dihydrogen orthophosphate solution of pH 2, 2.5, 3, 3.5, 4, 4.5, 5, 5.5, 6, 6.5, 7, 8, 9 and 10. It was found that the best-resolved anodic signal for oxidation of tetracycline was obtained at pH 2. Therefore, this pH was used for the rest of the experiments.

3.2. Cyclic voltammetry

The cyclic voltammetric (I–E) response is shown in Fig. 2 for the Au RDE in 0.1 M potassium dihydrogen orthophosphate solution with and without 1 mM tetracycline. The background response for the supporting electrolyte exhibits an anodic wave on the positive scan in the region of ca. +0.8 to +1.2 V versus Ag/AgCl (wave A). This background response corresponds to charging of the interfacial double layer and formation of a small amount of surface oxide. The cathodic peak obtained on the negative scan in the region of ca. +0.7 to +0.4 V versus Ag/AgCl (wave B) corresponds to dissolution of the surface oxide formed on the positive scan. In the presence of tetracycline, the two-step anodic signal for oxidation of tetracycline was observed on the positive scan beginning at ca. 0.6 V versus Ag/AgCl. The first and second steps was occurred in the region of ca. +0.6 to +0.9 V versus Ag/AgCl (wave C) and +0.95 to +1.15 V versus Ag/AgCl (wave D), respectively. The anodic response for tetracycline on the positive scan was sharply inhibited by the onset of surface oxide formation at potentials greater than ca. +1.2 V versus Ag/AgCl. The decrease of signal on the subsequent negative scan in the region of ca. +1.25 to +0.8 V versus Ag/AgCl indicates the reduction of activity for the oxide covered gold surface.

3.3. PAD waveform optimization

The PAD waveform used in this experiment is described in Fig. 1. E_{det} is the detection potential applied for the time period t_{det} ($t_{det} = t_{del} + t_{int}$), and the electrode current is sampled by electronic integration over the time period t_{int} following a delay of t_{del}

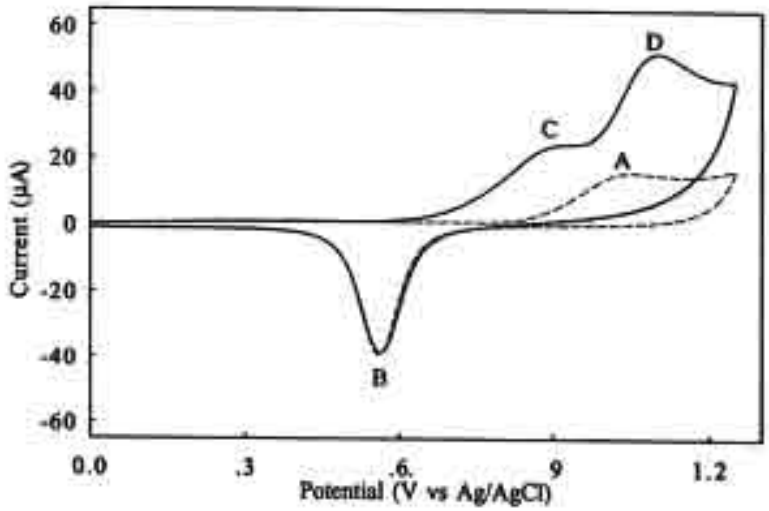

Fig. 2. Cyclic voltammetric response for 1 mM tetracycline in 0.1 M potassium dihydrogen orthophosphate solution (pH 2) at the Au RDE (0.07 cm^2). Condition: 250 rpm rotation speed; 50 mV s^{-1} scan rate. The background cyclic voltammogram is also shown (dash line).

to allow the charging current to diminish to a negligible value. A positive cleaning potential (E_{oxd}) that removes the oxidizable contaminant on the electrode surface is applied for the time period t_{oxd} following E_{det}. A negative reactivating potential (E_{red}) that dissolves the inert oxide product on the electrode surface is applied for the time period t_{red} following E_{oxd}. The optimization of each waveform parameter carried out in the FI system was studied while the other parameters were held constant. The average peak currents for each parameter were plotted versus the varied parameter. Observations of each parameter are discussed later.

3.4. Optimization of E_{det}, and t_{det}

Fig. 3a shows the FI–PAD response variations for 1 mM tetracycline according to E_{det} variation in the range +0.8 to +1.2 V versus Ag/AgCl in intervals of 0.5 V. The potential range used for E_{det} optimization was chosen from the potential region in the cyclic voltammogram (Fig. 2) where oxidation of tetracycline occurred. Clearly, the maximum current response is obtained at $E_{det} = 1.15$ V versus Ag/AgCl and application of this value in the PAD waveform was used. For this value, only a small contribution from surface oxide formation exists.

Fig. 3b shows the response for 1 mM tetracycline with t_{del} variation. It can be seen that the current is increased from 100 to 500 ms of delay time and the response decays beyond 500 ms. The t_{del} value of 500 ms is recommended as the optimal value.

Fig. 3c shows the FI–PAD response for 1 mM tetracycline with variation of t_{int} from 40 to 140 ms in intervals of 20 ms. On the basis of these results, a value of $t_{int} = 100$ ms was chosen as the optimal value.

3.5. Optimization of E_{oxd} and t_{oxd}

Fig. 3d shows the FI–PAD response for 1 mM tetracycline as a result of the variation of t_{oxd} from 30 to 180 ms at intervals of 30 ms for several values of E_{oxd} in the range +1.2 to +1.6 V versus Ag/AgCl in intervals of 0.1 V. The clean electrode becomes progressively fouled by the detection products during application of E_{det} and E_{oxd} was applied to clean the surface of electrode. For the values of E_{oxd} shown, the value of $t_{oxd} = 150$ ms is sufficient for the oxidative cleaning of the electrode surface. For each value of t_{oxd}, the highest current signals were obtained at $E_{oxd} = 1.6$ V versus Ag/AgCl. Hence, the values for $E_{oxd} = 1.6$ V versus Ag/AgCl and $t_{oxd} = 150$ ms are recommended as optimal.

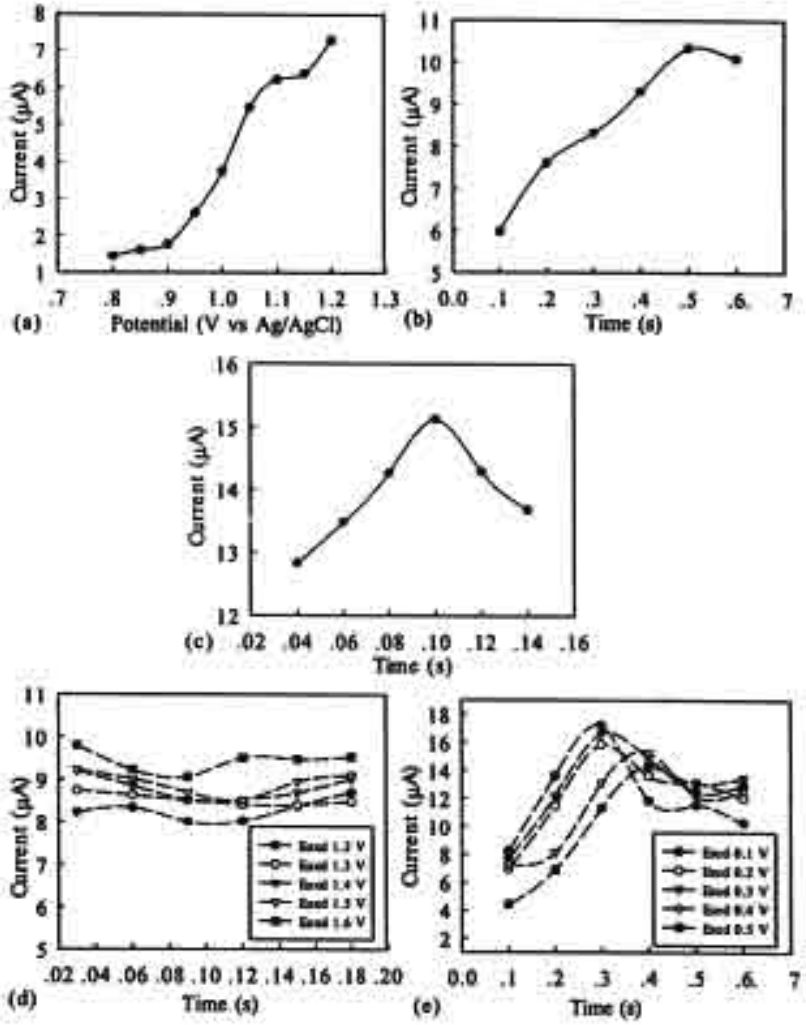

Fig. 3. FI–PAD response as a function of (a) E_{det}, (b) t_{det}, (c) t_{int}, (d) E_{oxd} and t_{oxd} and (e) E_{red} and t_{red} for tetracycline in 0.1 M potassium dihydrogen orthophosphate solution (pH 2) at the Au RDE (0.07 cm^2).

3.6. Optimization of E_{red} and t_{red}

The formation of surface oxide at the electrode surface, which reduced the electrode surface activity, occurred during the application of E_{oxd}. Therefore, it is essential that the values of E_{red} and t_{red} are chosen to achieve complete reductive dissolution of the surface oxide. Fig. 3e shows the FI–PAD response of 1 mM tetracycline with variation of t_{red} from 100 to 600 ms in intervals of 100 ms for several values of E_{red} in the range +0.1 to +0.5 V versus Ag/AgCl in intervals of 0.1 V. For the values of E_{red} shown, the highest current signals were obtained at the value of $t_{red} = 300$ ms. For each value of t_{red} +0.1 V is chosen as the optimum value for E_{red}. Therefore, the values of $E_{red} = 0.1$ V versus Ag/AgCl and $t_{red} = 300$ ms are recommended as the chosen values for the PAD waveform.

3.7. Linear range and the detection limit

Fig. 4 shows a series of repetitive 20 μl injections of tetracycline in 0.1 M potassium dihydrogen orthophosphate solution pH 2 under the optimized PAD waveform parameters described above. Well-defined signals

were obtained at all concentration from 5 μM to 2 mM. The current signal increased with increase in concentration. The calibration curve for tetracycline standard solutions was obtained from the pulsed amperometric responses. A linear response range between 5 μM and 0.6 mM tetracycline with sensitivity of 13.7 μA mM^{-1} and a correlation coefficient of 0.993 was obtained. The regression equation was $Y = 13.71X + 0.23$, where Y is the current response (μA) and X the concentration (mM). Interestingly, the detection with a S/N > 3 was obtained at a concentration of 1 μM of tetracycline.

3.8. Repeatability

The R.S.D. value was used to define the repeatability. Under the optimal PAD waveform parameters, a 0.5 mM of tetracycline solution in 0.1 M potassium hydrogen phosphate was injected 10 times at a flow rate of 1 ml min^{-1}. The %R.S.D., from the results was 3.5%.

3.9. Drug analysis of tetracycline capsules

The proposed PAD method for tetracycline was applied to the determination of tetracycline capsules. Using the regression equation (in linear range and the detection limit section) for the calibration plot, the amount of tetracycline hydrochloride was obtained to be a value of 254.3±9.3 mg per capsule ($n = 5$). Good agreement was obtained between the value obtained by the PAD method and the labeled value (250 mg per capsule). The anodic detection of tetracycline compound is concomitant with the anodic formation of oxide at the Au electrode and so could cause some error from interference products during the oxidative step. However, pulsed amperometric detection of tetracycline with FI still gives a low detection limit and a wide dynamic linear range.

4. Conclusion

This is the first investigation of tetracycline using pulsed amperometry applied to a flow injection system. The optimized conditions, such as pH and the various potentials were examined. The results show that FI–PAD with the optimized conditions can be used to determine tetracycline in the concentration range of 0.005–0.6 mM with a slope of 13.7 μA/mM. FI–PAD provided very low detection limit (10 ng). In comparison to the other amperometric method reported in the literature [18], this proposed method gives lower detection limit, wider working concentration range. The proposed method is simple and time saving because the cleaning step occurs simultaneously during the measurement. The determination of tetracycline in commercially available tablet dosage forms indicates that this proposed method is precise and accurate.

Acknowledgements

Acknowledgment is made to the Thailand Research Fund. Special thanks are extended to Asst. Prof. Dr. Duangjai Nacapricha (Mahidol University) and King Mongkut Univ. Technol. Thonburi, Sch Bioresources & Technol.

References

[1] S.M. Sultan, F.O. Suliman, S.O. Duffuaa, I.I. Abu-Abdoun, Analyst 117 (1992) 1179.
[2] R. Karlicek, P. Solich, Anal. Chim. Acta 285 (1994) 9.
[3] P. Izquierdo, A. Gomez-Hens, D. Perez-Bendito, Anal. Chim. Acta 292 (1994) 133.
[4] S. Croubels, C.V. Peteghem, W. Baeyens, Analyst 119 (1994) 2713.
[5] B. Gala, A. Gomez-Hens, D. Perez-Bendito, Talanta 44 (1997) 1883.
[6] A.L. Savage, S.H. Sarijo, J. Baird, Anal. Chim. Acta 375 (1998) 1.
[7] H.C. Goicoechea, A.C. Olivieri, Anal. Chem. 71 (1999) 4361.
[8] S.A. Halvatzis, M.M. Timotheou-Potamia, A.C. Calokerinos, Analyst 118 (1993) 633.
[9] X.R. Zhang, W.R.G. Baeyens, A. Van den Borre, G. Van der Weken, A.C. Calokerinos, S.G. Schulman, Analyst 120 (1995) 463.
[10] H. Han, Z. He, Y. Zeng, Anal. Sci. 15 (1999) 467.
[11] D.L. Collins-Thompson, D.S. Wood, I.Q. Thompson, J. Food Prot. 51 (1988) 632.
[12] E. D'Haese, H.J. Nelis, W. Reybroeck, Appl. Environ. Microbiol. 63 (1997) 4116.
[13] J. Kuriitu, S. Lonnberg, M. Virto, M. Karp, J. Agric. Food Chem. 48 (2000) 3372.
[14] S. Sabharwal, K. Kishore, P.N. Moorthy, J. Pharm. Sci. 77 (1988) 78.
[15] I. Tanase, I. David, G. Radu, E. Iorgulescu, V. Magearu, Analusis 24 (1996) 281.
[16] W. Hou, E. Wang, Analyst 114 (1989) 699.

[17] W. Oungpipat, P. Southwell-Keely, P.M. Alexander, Analyst 120 (1995) 1559.
[18] H. Ji, E. Wang, Analyst 113 (1988) 1541.
[19] A.G. Kazemifard, D.E. Moore, J. Pharm. Biomed. Anal. 16 (1997) 689.
[20] A. Inoue, R.L. Earley, M.W. Lehmann, L.E. Welch, Talanta 46 (1998) 1507.
[21] D.C. Johnson, W.R. LaCourse, Anal. Chem. 62 (1990) 589A.
[22] W.R. LaCourse, D.A. Mead Jr., D.C. Johnson, Anal. Chem. 62 (1990) 220.
[23] W.R. LaCourse, D.C. Johnson, Carbohydr. Res. 215 (1991) 159.
[24] R.L. Earley, J.S. Miller, L.E. Welch, Talanta 45 (1998) 1255.
[25] R.W. Andrews, R.M. King, Anal. Chem. 62 (1990) 2130.
[26] D.G. Williams, D.C. Johnson, Anal. Chem. 64 (1992) 1785.
[27] P.J. Vandeberg, D.C. Johnson, Anal. Chim. Acta 290 (1994) 317.
[28] J. Lee, S. Mho, C.H. Pyun, I. Yen, Bull. Korean Chem. Soc. 15 (1994) 1038.
[29] G. Schiavon, N. Comisso, R. Toniolo, G. Bontempelli, Electroanalysis 8 (1996) 544.
[30] S. Park, S. Hong, J. You, Bull. Korean Chem. Soc. 17 (1996) 143.
[31] M.W. Lehmann, M.R. Fahr, L.E. Welch, Talanta 44 (1997) 1231.
[32] C.O. Dasenbrock, W.R. LaCourse, Anal. Chem. 70 (1998) 2415.
[33] A.P. Clarke, P. Jandik, R.D. Rocklin, Y. Liu, N. Avdalovic, Anal. Chem. 71 (1999) 2774.
[34] T.R.I. Cataldi, C. Campa, G.E. De Benedetto, Fresenius J. Anal. Chem. 368 (2000) 739.
[35] G. Weber, Fresenius J. Anal. Chem. 356 (1996) 242.
[36] X.W. Zheng, Y. Mei, Z.J. Zhang, Anal. Chim. Acta 440 (2001) 143.
[37] M.G.F. Sales, M. Montenegro, J. Pharm. Biomed. Anal. 90 (2001) 1125.

Available online at www.sciencedirect.com
SCIENCE DIRECT®
Analytica Chimica Acta 499 (2003) 167–172
ANALYTICA CHIMICA ACTA
www.elsevier.com/locate/aca

Exploiting sequential injection analysis with bead injection and lab-on-valve for determination of lead using electrothermal atomic absorption spectrometry

Pattanapong Ampan[a], Jaromir Ruzicka[b], Raja Atallah[c], Gary D. Christian[b,*], Jaroon Jakmunee[a], Kate Grudpan[a]

[a] Department of Chemistry, Faculty of Science, Chiang Mai University, Chiang Mai 50200, Thailand
[b] Department of Chemistry, University of Washington, Box 351700, Seattle, WA 98195-1700, USA
[c] Department of Environmental Health, University of Washington, Box 357234, Seattle, WA 98195-7234, USA

Received 2 April 2003; received in revised form 16 July 2003; accepted 4 August 2003

Abstract

Sequential injection (SI) with bead injection (BI) and lab-on-valve (L-O-V) was exploited for determination of trace lead using electrothermal atomic absorption spectrometry (ETAAS). A renewable microcolumn incorporated within the L-O-V system was investigated by using Sephadex G-25 impregnated by dithizone. Lead solution was passed through the impregnated beads. The beads were directly propelled into a graphite tube where they were pyrolyzed and lead ions were subsequently atomized. Conditions of the ETAAS measurement were studied including chemical modifiers (palladium, molybdenum and tartaric acid). The SI system for trapping of lead on the beads in the L-O-V could be operated in parallel to the ETAAS operation.

Keywords: Sequential injection; Bead injection; Lead; Electrothermal atomic absorption spectrometry

1. Introduction

Electrothermal atomic absorption spectrometry (ETAAS) is conventionally employed for trace metal analysis. Lead has been assayed in application to various types of samples, such as wine [1], sugars [2], fish samples [3], and blood [4,5]. Effects due to the matrix of samples must usually be eliminated. Besides addition of matrix modifiers, sample-pretreatment using column techniques has been widely used. Flow injection-ETAAS has been achieved for determination of lead in many kinds of samples, such as estuarine water and fertilizers [6], blood samples [7], and some high-purity reagents [8].

FI minicolumns (in-valve or in-line) are useful, but factors such as column back-pressure, efficiency of eluent, eluent volume, and elution time must be dealt with, and may influence precision and accuracy. Sequential injection (SI) was first introduced to reduce reagent consumption and perform operations readily with automation via a computer [9].

SI with a bead injection (BI) renewable microcolumn for preconcentration and pre-separation has been used for determination of copper [10]. The measurement is carried out after the analyte is sorbed onto beads, and then the used beads are discarded. A

* Corresponding author. Tel.: +1-206-543-1635; fax: +1-206-685-3478.
E-mail address: christian@cbem.washington.edu (G.D. Christian).

0003-2670/$ – see front matter © 2003 Elsevier B.V. All rights reserved.
doi:10.1016/j.aca.2003.08.030

renewable microcolumn loaded with SP Sephadex C-25 cation exchange resin was used for on-line preconcentration and separation before determination of nickel by ETAAS [11,12]. The ion sorbed beads [11] or the eluate from the beads [12] could be transferred into the graphite atomizer. A similar system was applied for the determination of trace bismuth in urine and river sediment [13].

In this paper, attempts were made to exploit SI with BI and the lab-on-valve (L-O-V) [14] for sample-pretreatment for trace lead determination using beads (Sephadex G-25 impregnated with dithizone) as renewable carrier. The bead sorbed lead was directly transported into the graphite atomizer.

2. Experimental

2.1. Instrumentation

A Perkin-Elmer Model 5100 PC atomic absorption spectrometer equipped with Zeeman background correction (Perkin-Elmer, Norwalk, CT, USA) with an AS-60 autosampler and HGA-600 graphite furnace were employed. Measurements were performed using a hollow cathode lamp operated at a wavelength of 283.3 nm, with a bandwidth of 0.7 nm and a current of 14 mA. A pyrolytic graphite platform was used for atomization. Argon served as the inert gas at 300 ml min^{-1}, except in the atomization step during which the flow was halted.

The ETAAS was coupled with an SI system (FIAlab-3500, FIAlab Instruments, Medina, WA, USA) consisting of a syringe pump (1000 μl volume), a six-port selection valve, and a unidirectional peristaltic mini-pump. The six-port selection valve was mounted with an L-O-V, which served as an integrated microsystem for this application (see Fig. 1).

The L-O-V was designed to match a six-port valve. This unit was made of Perspex (diameter 50 mm, thickness 10 mm), having five ports and one-flow-through port, in addition to in and out ports for loading the sample. Two of the channels served as microcolumns (referred to as C1 and C2 in Fig. 1 and Table 1). The outlets of these channels were inserted with rods, small pieces of rigid PEEK tubing, id 0.0635 mm (Upchurch, part number 1560), in order to entrap beads into the channel but to allow liquid through. (See Refs. [11–13] and http://www.flowinjection.com for further details of the L-O-V and BI system.)

2.2. Chemicals and reagents

All reagents were of analytical grade. A series of lead standard solutions was prepared from 1000 μg ml^{-1} lead standard, AAS grade (Merck, Germany). Beads were of Sephadex G-25, 50–150 μm

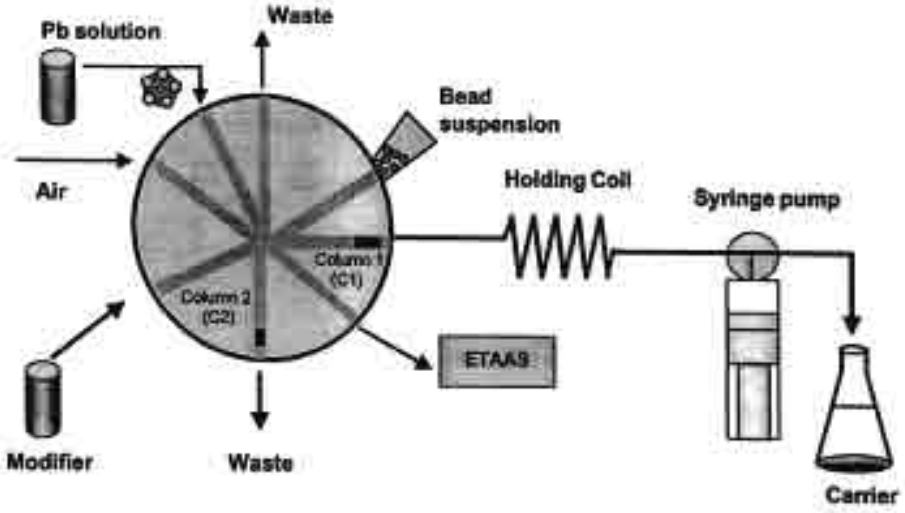

Fig. 1. SI system with L-O-V device mounted on the selection valve.

Table 1
Sequence of operating of the selection valve (SL valve), the syringe-pump valve (SP valve), and sample/reagents for 500 μl of sample loading

Step	Description	Port of SP valve	Port of SL valve	Flow rate (μl/s)	Action of flow	Volume (μl)
1	Washing					
	(a) Empty column 2 (C2)	Out	Column 2	25	Dispense	Empty
	(b) Fill syringe	In	Column 2	200	Aspirate	750
	(c) Washing C2	Out	Column 2	100	Dispense	650
2	Introducing beads					
	(a) Beads to column 1 (C1) (preventing to HC)	Out	Bead	10	Aspirate	10
	(b) Beads from C1 to C2	Out	Column 2	10	Dispense	100
3	Filling carrier	In	Column 2	200	Aspirate	400
4	Preconcentration					
	(a) sample into HC	Out	Std/sample	200	Aspirate	500
	(b) Sample passing through beads in column 2	Out	Column 2	10	Dispense	500
5	Washing sample behind C2					
	(a) Inserting air	Out	Air	100	Aspirate	50
	(b) Washing column 2	Out	Column 2	10	Dispense	50
6	Getting air	Out	Air	50	Aspirate	500
7	Drawing beads	Out	Column 2	200	Aspirate	100
8	Filling modifiers	Out	Modifier	10	Aspirate	10
9	Sending beads	Out	Detector	200	Dispense	100
		Out	Detector	50	Dispense	400

(SIGMA, USA). Dithiophenylcarbazone (Merck, Germany) was prepared in pH 12 solution (Table 4).

2.3. Procedure

The sequence for the SI–BI–L-O-V system was performed using a software "Program A", as summarized in Table 1. A mini-motor stirrer was used to assist homogenizing the bead suspension (1:20) during the bead introduction into the system. The conditions and temperature program of the ETAAS measurement are shown in Table 2.

Table 2
The graphite furnace program for determination of lead with Sephadex G-25 beads

Step	Temperature (°C)	Ramp time (s)	Hold time (s)	Argon flow rate ($ml\,min^{-1}$)
Preheating	70	5	10	300
Drying-1	120	1	10	300
Drying-2	300	10	20	300
Pyrolysis	1200	20	40	300
Cooling	20	1	15	300
Atomization	1800	0	5	0
Cleaning	2600	1	5	300

The cycle was set so that when the beads with the sorbed lead had just been introduced into the graphite tube of the ETAAS, the next sample-pretreatment by the SI system was started in parallel to the ETAAS detection process.

3. Results and discussion

3.1. Optimization of conditions

Because the lead sorbed on Sephadex is to be detected by ETAAS, lead measurement with the beads as matrix was investigated. During the atomization step, the beads should be sufficiently decomposed, to decrease the background signal due to the beads.

The effect of the pyrolysis temperature was studied by starting at a temperature of 850 °C and using $Mg(NO_3)_2$ and $NH_4H_2PO_4$ as chemical modifiers, which are recommended by the manufacturer for a sample with organic matter. The results (in Fig. 2) indicated that 1050 °C should be used, but high background was still observed. The temperature of 1200 °C would be preferred, but the lead is lost. The effect of pyrolysis time was then investigated for the

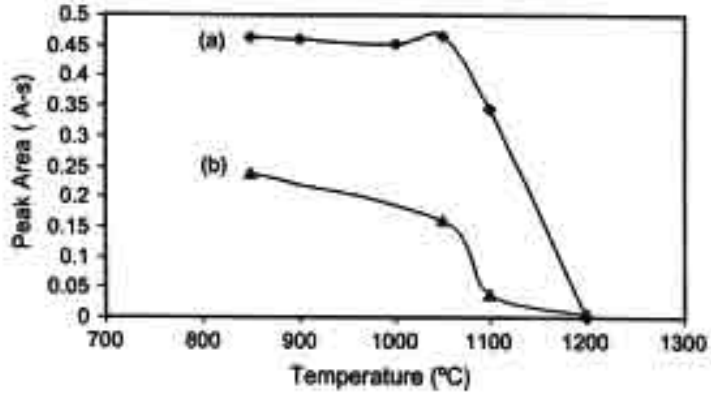

Fig. 2. Effect of pyrolysis temperature (pyrolysis time of 40 s): (a) 2 ng Pb-sorbed on beads; (b) beads alone.

temperature of 1050 °C. The results (Fig. 3) indicated that prolonged pyrolysis time resulted in loss of lead.

Various chemical modifiers (Table 3) were then considered, to suppress loss of lead, employing a pyrolysis time of 40 s. This time assured adequate pyrolysis and recovery under the optimum conditions. While we did not explore shorter pyrolysis times, it is possible pyrolysis can be achieved with somewhat shorter times. Under pyrolysis at 850 °C using magnesium chloride and ammonium dihydrogen phosphate as modifiers (lower temperature conditions) it was observed that carbonaceous residue built up on the graphite tube. For the lower temperature conditions, the lifetime of a graphite tube was about 20 runs whereas it was roughly 40 runs for the higher temperature conditions (1200 °C with modifiers used). It was found that a mixture of palladium chloride, ammonium heptamolybdate and sodium tartrate (3 μg:20 μg:400 μg) should be the most appropriate, as it resulted in the lowest background, the least loss, and longer lifetime of the graphite tube. With this, the recovery of 2 ng lead was 95% and the net background signal was 0.012 compared to 0.1 for the lead. The H_2O_2 and HNO_3 mixture, which was suitable to determination of Pb in honey [15], was not satisfactory here. Pd has been employed in lead determination in honey [15], blood and urine [16], and geological samples [17,18], but Pd alone was not suitable here either. Neither was its mixture with H_2O_2.

The effects of loading flow rate and the flow rate for bead transfer were investigated. High flow rates for loading may cause beads to escape from the cell

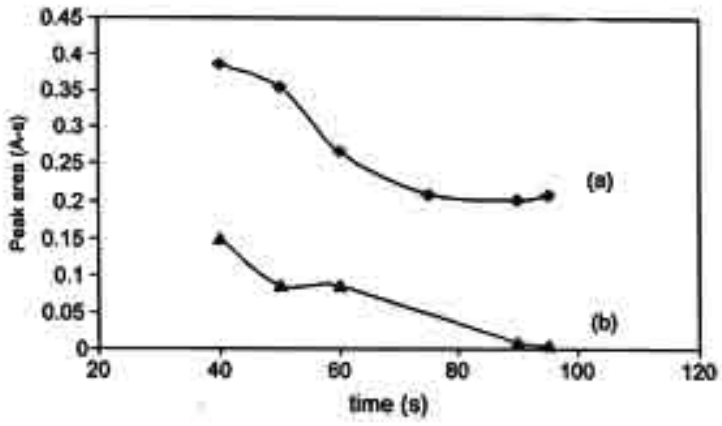

Fig. 3. Effect of pyrolysis time (pyrolysis temperature of 1050 °C): (a) 2 ng Pb sorbed on beads; (b) beads alone.

Table 3
Determination of lead added (2 ng) onto Sephadex beads in the presence of various modifiers

Modifiers (in 10 μl)	Pyrolysis temperature (°C)	Background signal (Abs-s)	Lead found (ng)	Relative loss (%)
$Mg(NO_3)_2$ (0.01 mg) + $NH_4H_2PO_4$ (0.2 mg)	850	0.036	1.9	5
H_2O_2 (3%, v/v)	850	0	1.0	50
H_2O_2 (3%, v/v) + HNO_3 (1%, w/v)	850	0.01	1.1	45
$Mg(NO_3)_2$ (0.01 mg) + $NH_4H_2PO_4$ (0.2 mg) + H_2O_2 (3%, v/v)	850	0.042	1.8	10
$PdCl_2$ (3 μg)	1200	0.025	1.8	10
$PdCl_2$ (3 μg) + H_2O_2 (3%, v/v)	1200	0.019	1.7	15
$PdCl_2$ (3 μg) + $(NH_4)_6Mo_7O_{24}$ (20 μg) + $C_4H_4Na_2O_6$ (400 μg)	1200	0.012	1.9	5
$PdCl_2$ (3 μg) + $(NH_4)_6Mo_7O_{24}$ (20 μg) + $C_4H_4Na_2O_6$ (400 μg) + H_2O_2 (3%, v/v)	1200	0.057	1.8	10

(microcolumn) via the very small space between a column plug and the inner wall of the channel of the L-O-V [14]. No significant difference was found for a loading flow rate of 1–20 $\mu l\,s^{-1}$ (step 4(b) in Table 1). The flow rate for transferring beads from the cell (column 1) of the L-O-V to the ETAAS was 200 $\mu l\,s^{-1}$, followed by 50 $\mu l\,s^{-1}$ as they reached the atomizer.

The choice of buffer and effect of pH of the carrier were studied. Tartrate buffer should not be used because tartrate is one of the chemical modifiers used, and the amount of tartrate would affect the signal obtained. Potassium hydrogen phthalate (KHP) was employed in this work by using a carrier with various compositions for pH 3–5 as described in Table 4. It was found that pH of the carrier was critical. A carrier of phthalate buffer with pH 5 gave the highest signal (orange color of beads was observed) (Fig. 4). By using buffer pH <5 as carrier, the signals tremendously deteriorated (purple color of beads was observed) and the signals decreased when using buffer pH >5 as carrier (with an observed diminishing of the orange color of the beads). Therefore the phthalate buffer pH 5 was selected.

Table 4
Preparation of buffer solutions with various pH values by mixing solutions A and B [18]

pH	Solution A	Solution B
1	25 ml of 0.2 M KCl	67.0 ml of 0.2 M HCl
2	25 ml of 0.2 M KCl	6.5 ml of 0.2 M HCl
3	50 ml of 0.1 M KHP	22.3 ml of 0.1 M HCl
4	50 ml of 0.1 M KHP	0.1 ml of 0.1 M HCl
5	50 ml of 0.1 M KHP	22.6 ml of 0.1 M NaOH
6	50 ml of 0.1 M KH_2PO_4	5.6 ml of 0.1 M NaOH
7	50 ml of 0.1 M KH_2PO_4	29.1 ml of 0.1 M NaOH
8	50 ml of 0.1 M KH_2PO_4	46.1 ml of 0.1 M NaOH
9	50 ml of 0.025 M borax	4.6 ml of 0.2 M HCl
10	50 ml of 0.025 M borax	18.3 ml of 0.1 M NaOH
11	50 ml of 0.05 M Na_2HPO_4	4.1 ml of 0.1 M NaOH
12	25 ml of 0.2 M KCl	6.0 ml of 0.2 M NaOH

A study on the effect of pH of the standard solution (prepared in the buffers listed in Table 4) was made. No significant effect of pH of the standard solution (pH 3–8) was found when using the phthalate buffer at pH 5 as carrier.

Dithizone was selected as the chelating agent for concentrating lead since it is a common reagent for the solvent extraction of lead [19]. A potential advantage of using a chelating agent in lieu of cation exchange is less effect of high concentrations of other cations, e.g., sodium, on the equilibrium. The effect of dithizone concentration was investigated. Sephadex G-25 beads were soaked in dithizone at pH 12, then equilibrated

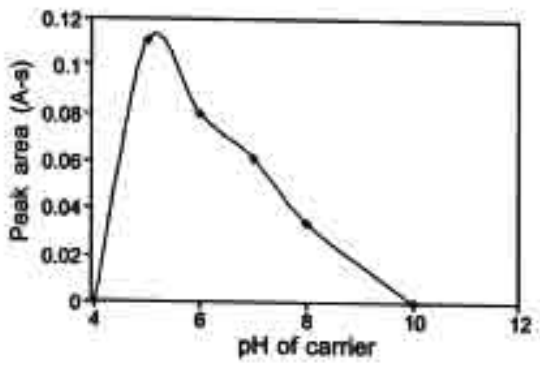

Fig. 4. Effect of pH of carrier.

at ambient temperature and kept in a photo-protected area for 30 min. The impregnated beads had to be freshly prepared. A suitable concentration of dithizone was 0.01% (w/v). The lead responses obtained from using various concentrations of dithizone (0.004, 0.01, 0.03, and 0.05%, w/v) were not significantly different. At 0.01% dithizone, it was easily sorbed in a reasonable time and the intensity of the dye was not too pale, assuring by visual inspection that an adequate amount had been sorbed.

3.2. Calibration

Using the proposed conditions of the ETAAS and SI system, a single standard calibration graph (plot of ng vs peak area) was obtained by loading 10 $\mu g\,l^{-1}$ Pb in pH 5 buffer with different loading times (100, 200, 400 μl; $Y = 0.082X - 0.047$; $R^2 = 0.992$). Loading 2000 μl of 1 and 2 $\mu g\,l^{-1}$ yielded the same results as loading 10 $\mu g\,l^{-1}$ for the same amount of Pb (ng). The linear regression line was: $Y = 0.080X - 0.052$; $R^2 = 0.991$. The relative standard deviation for 2 ng was 1.9% ($n = 3$). The detection limit was estimated at 0.3 ng (signal three times the standard deviation of the blank). The measured working range was 1–4 ng, which can be adjusted by the volume of sample loaded. The enrichment factor was 39. The detection limit is about an order of magnitude higher than the 0.02 ng obtained by Wang and Hansen [11] for nickel with an enrichment factor of 72. The difference was probably due to differences in backgrounds as well as in enrichment factors for the different elements.

4. Conclusion

A SI–BI–L-O-V system was exploited to determine trace lead by sorbing the lead on to microbeads for ETAAS measurement. Dithizone impregnated Sephadex G-25 beads were employed in a renewable microcolumn in the L-O-V system. The Pb-sorbed beads were directly transferred from the L-O-V into a graphite tube of the ETAAS where beads were pyrolyzed and lead ions were atomized subsequently, using a pyrolysis temperature of 1200 °C for 40 s, with chemical modifiers (Pd, Mo, and tartaric acid).

The SI–BI–L-O-V process for lead sorption onto the beads could be run in parallel to the ETAAS operation. This leads to a high sample throughput (12 determinations h^{-1}). This system should allow rapid separation and preconcentration of lead from samples with high matrix background.

Acknowledgements

Thanks are due to the Thailand Research Fund (TRF), and especially the Royal Golden Jubilee (RGJ) scholarship to PA, and partial support from the Postgraduate Education and Research Program in Chemistry (PERCH). The Department of Chemistry and the Environmental Health Laboratory, University of Washington are acknowledged for providing the facilities.

References

[1] L. Jorhem, B. Sundstrom, Atom. Spectrosc. 16 (1995) 226.
[2] N.J. Miller-Ihli, F.E. Greene, Atom. Spectrosc. 14 (1993) 85.
[3] S.J. Huang, S.J. Jiang, Analyst 125 (2000) 1491.
[4] C.P. Bosnak, D. Bradshaw, R. Hergenreder, K. Kingston, Atom. Spectrosc. 14 (1993) 80.
[5] J.A. Navarro, V.A. Granadillo, O.E. Parra, R.A. Romero, J. Anal. Atom. Spectrom. 4 (1989) 401.
[6] R. Ma, W. Van Mol, F. Adams, Atom. Spectrosc. 17 (1996) 176.
[7] E. Ivanova, W. van Mol, F. Adams, Spectrochim. Acta B 53 (1998) 1041.
[8] M. Sperling, X.P. Yan, B. Welz, Spectrochim. Acta B 51 (1996) 1875.
[9] J. Ruzicka, G.D. Marshall, Anal. Chim. Acta 237 (1990) 329.
[10] C.C. Oliveira, E.A.G. Zagatto, J. Ruzicka, G.D. Christian, Anal Lett. 33 (2000) 929.
[11] J. Wang, E.H. Hansen, Anal. Chim. Acta 424 (2000) 223.
[12] J. Wang, E.H. Hansen, Anal. Chim. Acta 435 (2001) 331.
[13] J. Wang, E.H. Hansen, Atom. Spectrosc. 22 (2001) 312.
[14] J. Ruzicka, Analyst 125 (2000) 1053.
[15] P. Vinas, I. Lopez-Garcia, M. Lanzon, M. Hernandez-Cordoba, J. Agric. Food Chem. 45 (1997) 3952.
[16] J.L. Buguera, M. Burguera, C.E. Rondon, Atom. Spectrosc. 18 (1997) 109.
[17] O. Acar, A. Rehber Tuker, Z. Kilic, Fresen. J. Anal. Chem. 357 (1997) 656.
[18] O. Acar, A. Rehber Tuker, Z. Kilic, Fresen. J. Anal. Chem. 360 (1998) 645.
[19] G.H. Morrison, H. Freiser, Solvent Extraction in Analytical Chemistry, Wiley, New York, 1957.

ANALYTICAL SCIENCES NOVEMBER 2003, VOL. 19

A Low-Cost Light-Scattering Detector for the Flow-Injection Nephelometric Determination of Sulfate

Jaroon JAKMUNEE,*1,*2† Yuthpong UDNAN,*1 Richard MORRISON,*3 Ronald BECKETT,*3,*4 Ian MCKINNON,*3 and Kate GRUDPAN*1,*2

*1 *Department of Chemistry, Faculty of Science, Chiang Mai University, Chiang Mai 50200, Thailand*
*2 *Institute for Science and Technology Research and Development, Chiang Mai University, Chiang Mai 50200, Thailand*
*3 *School of Chemistry, Monash University, Clayton, Victoria 3800, Australia*
*4 *Water Studies Centre, Monash University, Clayton, Victoria 3800, Australia*

A simple low-cost flow-through light-scattering detector was developed for determining the particle mass concentration in colloidal suspensions. Employing a laser pointer as a light source and a photodiode IC as a light sensor, the detector was shown to have good sensitivity, yet was small and battery operated. The detector was demonstrated to be effective for the flow-injection nephelometric determination of sulfate by precipitation as barium sulfate.

(Received July 23, 2003, Accepted August 13, 2003)

Introduction

Light-scattering detection has been applied in flow analysis for either the determination of size or mass concentration of particles.[1] Multiangle light-scattering detectors can be combined with particle separation techniques, such as field-flow fractionation (FFF)[2] and size-exclusion chromatography (SEC),[3] for size characterization. The mass concentration of particles can be determined by either multiangle or simple uniangle detectors.

The determination of a single analyte by uniangle light-scattering detection in flow injection (FI) and sequential injection (SI) analysis has been widely investigated. Either nephelometric (detection of scattered light at an angle of 90° to the incident beam) or turbidimetric (detection at 0°) methods are usually used. Although turbidity can be easily measured using a spectrophotometer, other phenomena (*e.g.* light absorption or light diffraction) may interfere. Nephelometric measurements are also more sensitive than turbidimetric measurements.

An SI system for the determination of chloride based on precipitation with silver ions has been proposed.[4] Phosphate can be determined by an SI turbidimetric method based on calcium phosphate precipitation.[5] A stopped FI turbidimetric immunoassay using the interaction of concanavalin A (antibody) and yeast mannan (antigen) has been investigated.[6] FI systems based on precipitation reactions have also been widely applied for the determination of drugs, such as thiamine,[7] promethazine,[8] amitriptyline,[9] and chlorhexidine.[10]

The determination of sulfate using barium chloride as a precipitating agent has previously been applied in both FI[11-14] and SI[15,16] systems. A liquid-drop windowless optical cell has been developed for FI turbidimetric or nephelometric determination of sulfate by precipitation with barium ion.[17]

In this work, a simple and low-cost flow-through light scattering detection system for determining the particle mass concentration was developed. It is based on nephelometric detection, using a laser pointer as a light source and a photodiode IC as a light sensor. The detector was utilized for the flow injection determination of sulfate by precipitation as barium sulfate.

Experimental

Chemicals

Deionized water (Milli Q, Millipore) was used throughout. All reagents were of analytical grade, unless otherwise stated. Sodium sulfate (Merck) was used to prepare a standard sulfate stock solution of 1000 mg SO_4^{2-}/L. Solutions of 1.2% w/v $BaCl_2$ and 0.1% w/v polyvinyl alcohol (PVA) in 0.05 M HCl were prepared from chemicals from Merck. Ethylenediaminetetraacetic acid disodium salt (Na_2EDTA, Merck) was used to prepare 0.2% w/v EDTA. A polystyrene latex bead suspension (particle diameter 0.144 μm) was obtained from Seradyn (IN, USA).

Flow injection apparatus

The flow-injection system used for the determination of sulfate is illustrated in Fig. 1. The system was assembled using a peristaltic pump (FIAlab Instruments, USA), a 6-port injection valve (Upchurch Scientific, USA), a 100 cm mixing coil and a flow-through light-scattering cell with a home-built detection system. All connections were made with 0.8 mm i.d. PTFE tubing.

Light scattering detector

A cross-section of the cell is shown in Fig. 2. A perspex plastic block was drilled in order to insert a straight glass tube

† To whom correspondence should be addressed.
E-mail: scijjkmn@chiangmai.ac.th

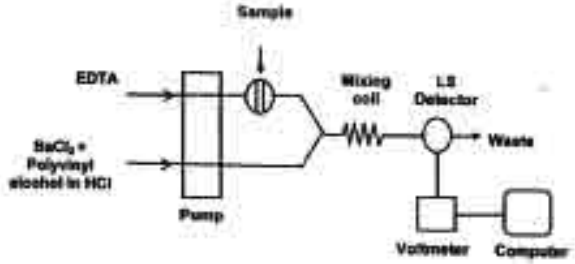

Fig. 1 Flow-injection nephelometric system for the determination of sulfate. Solutions were 0.2% w/v EDTA (or 0.0060 M) and 1.2% w/v $BaCl_2$ (or 0.058 M) plus 0.1% w/v PVA in 0.05 M HCl.

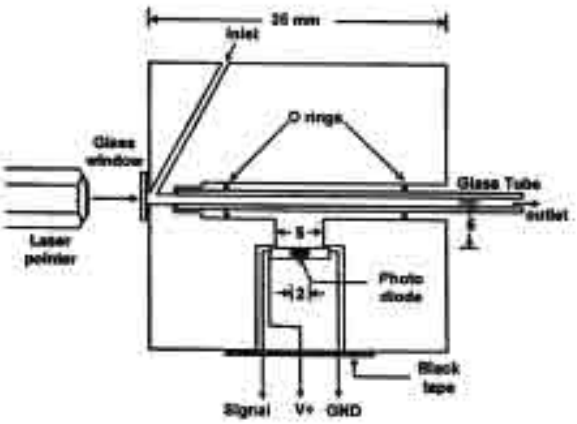

Fig. 2 Schematic diagram of the flow-through light scattering cell.

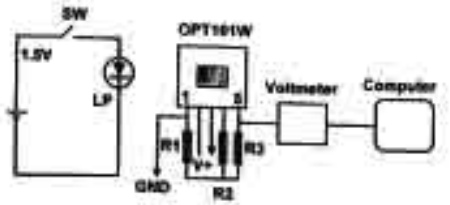

Fig. 3 Light-scattering detector circuit. R1, R2 and R3 are resistors of 3.3 kΩ, 10 MΩ, 100 kΩ, respectively.

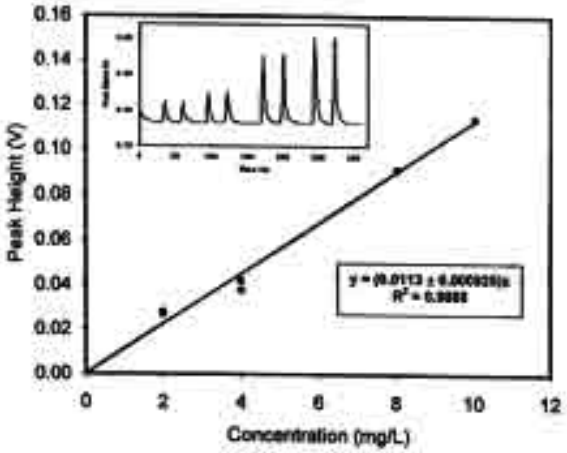

Fig. 4 Calibration plot of the detector voltage *versus* the polystyrene (monodisperse 0.144 μm beads) concentration fitted to a straight line through the origin.

(2 mm i.d.) with o-ring sealing. A light sensor (described below) was mounted at right angles to the tube axis, as shown. A glass microscope cover slide, attached to the block using epoxy glue, acted as a window and sealed the flow-through cell. The block was painted black to minimize any stray light. Finally, the flow cell, the light source and the detector were placed inside a black box

The detection system is depicted in Fig. 3. A red laser diode pointer (680 nm) was used as a light source. A 1.5 V AAA size alkaline battery was sufficient to power the laser diode for at least 3 h. The optical sensor which converts light intensity to voltage was an OPT101W (Burr-Brown Corporation), which has an active area of 2.3 × 2.3 mm and a peak spectral response at 850 nm, where the responsivity was 0.6 A/W. The useable working range of this detector was 300 nm to 1 μm.

The OPT101W is housed in a 5-pin, single, in-line package (SIP) containing an integral photodiode and current amplifier. Three external resistors, connected in a "tee" network, were added, as shown in Fig. 3. This configuration[18] results in an effective feedback resistance exceeding 300 MW, giving an effective gain of 3×10^8 V/A. While the frequency response of the detector is significantly reduced when operating at such a high gain, we estimate its value to be about 40 - 50 Hz, which is more than adequate for the experiments described here. The output of the OPT101W appears as a voltage on pin 5, which was measured by a digital multimeter (Dick Smith Electronics, Australia) interfaced to a computer (Compaq, USA).

Owing to the high circuit gain the input offset current of the OPT101W's internal op-amp produces a small, constant offset voltage (<100 mV) that contributes to the baseline signals in the experiments reported here.

As shown in Fig. 2, the 2.3 mm square detector is positioned 5 mm from the center of the glass tube through which samples flow. This geometry results in the collection of light scattered through the range 90 ± 40°. Experiments performed using a much smaller aperture (2 mm) immediately in front of the detector resulted in much weaker signals. The use of a higher powered light source would allow the collection angle to be better defined while maintaining a useful scattering signal.

Procedure for sulfate analysis

A standard or sample (100 μL) was injected into a stream of 0.2% w/v EDTA pumped at 1.5 mL/min using a peristaltic pump (see Fig. 1), which then passed through a mixing coil to merge with a stream of 1.2% w/v $BaCl_2$ and 0.1% w/v polyvinyl alcohol (PVA) in 0.05 M HCl before entering the flow-through cell. Light scattering caused by the barium sulfate precipitate was monitored by the detector and recorded on a computer. An FIAgram (a plot of output voltage (linearly proportional to the light scattering intensity) *vs.* time) was obtained for each injection. Data for a series of standard sulfate solutions were plotted (peak height *versus* sulfate concentration), and the resulting calibration graph was used to determine the concentration of sulfate in the unknown water samples.

Results and Discussion

Testing of FI-LSD instrument

A series of 0.144 μm polystyrene (PS) latex suspensions with concentrations in the range of 2 – 10 mg/L were injected into the FI system and allowed to flow-through the LS detector. The

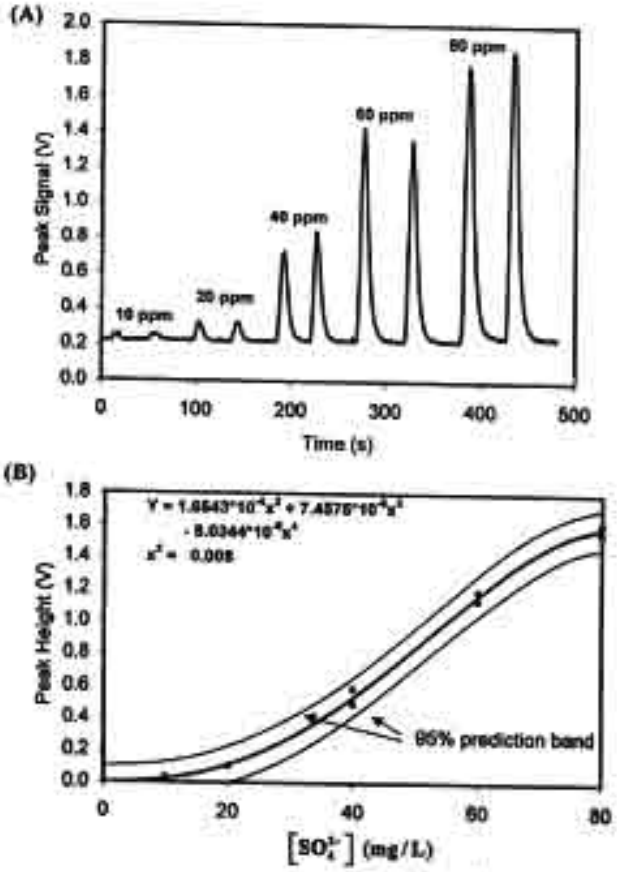

Fig. 5 (A) FIAgrams obtained with the FIA-LS system shown in Fig. 1 using 100 µL injections of sulfate of various concentrations. (B) Calibration plot of the detector voltage *versus* the sulfate concentration fitted to a truncated quartic equation, as explained in the text. x^2 = sum of squares of deviations of the points from the line. 95% prediction band such that 95% of the measured points are expected to lie within the band.

maximum difference between replicates of the resulting FIAgrams (detector voltage *versus* time) was 10%. The pooled standard deviation between replicates was 1 mV or 2% at the mid-range of the data. The resultant calibration line is plotted in Fig. 4. The data demonstrate the linearity of the detection system. The uncertainty in the slope of the line (the standard error as determined by a least-squares fitting procedure), was ±1%.

Flow-injection nephelometric determination of sulfate

Using the FI manifold shown in Fig. 1, the effects of various measurement conditions, concentrations of reagents (EDTA, $BaCl_2$, polyvinyl alcohol), flow rates, injection volume and mixing coil length were studied. From this information the run conditions selected were: Na_2EDTA concentration 0.2% (w/v) or 0.0060 M, $BaCl_2$ concentration 1.2% (w/v) or 0.058 M, PVA concentration 0.1% (w/v), sample injection volume 100 µL, mixing coil length 100 cm and flow rate for each line 1.5 mL/min.

The carrier stream of alkaline EDTA acts as a wash solution as well as binding some metal ions in the sample.[14] Sulfate reacts with the excess barium ions to form a precipitate before reaching the light-scattering cell. The polyvinyl alcohol would help to stabilize the precipitate by forming a protective layer on the particles.

Table 1 Sulfate contents of natural water samples using the FIA-LS system

Sample	Peak height/V			Sulfate/mg L^{-1}	
	(i)	(ii)	Mean	Mean	95% confidence
A	0.378	0.362	0.370	30.3	±3
B	0.614	0.511	0.5625	41.8	±3
C	1.005	1.14	1.0725	58.7	±3
D	0.138	0.124	0.131	19.1	±6
E	0.549	0.491	0.52	34.8	±3
F	0.189	0.189	0.189	21.1	±5
G	0.104	0.102	0.103	18.7	±9

The FIAgrams obtained for a series of sulfate injections in the concentration range 10 – 80 mg/L are shown in Fig. 5A. No baseline drift was observed for at least 50 injections. The reproducibility of the peak heights was generally not as good as that for the PS latex sample, with the maximum variation between replicates being 17% and the pooled standard deviation ($f = 5$) over all the samples being 40 mV or 10% at mid-range. This may be due to the variation in the particle size of the precipitate formed, which would affect the scattering of light.[14]

The data are plotted in Fig. 5B and are clearly nonlinear. In the absence of any theoretical model for describing the non-linearity, several functions (exponential, sigmoid, polynomial) were evaluated (using the software package Igor Pro[15]) for use as an interpolation function. The simplest function that adequately represented the data was a truncated quartic,

$$y = k2x2 + k3x3 + k4x4, \quad (1)$$

The fitted curve is shown in Fig. 5B together with the prediction bands drawn such that 95% of measured points are expected to lie within the band.

The FIA-LS system was then utilized to analyze sulfate in some natural water samples. The reproducibility is similar to that of the sulfate standards: the maximum difference between replicates was 0.1 V or 17% and the pooled standard deviation over all the samples was 0.05 V ($f = 7$).

Using the quartic calibration curve obtained with the sulfate standards, the concentration of sulfate in each natural water was estimated. The results are given in Table 1 together with the 95% confidence limits, determined as follows.

$$95\%\ \text{confidence limit} = 0.5 \times \text{the width of the 95\% prediction band}/(\text{number of replicates})^{1/2} \quad (2)$$

Conclusion

A simple low-cost flow-through light scattering detector was developed for use in FI systems, where precipitates are generated and the resulting turbidity is used as the basis for chemical analysis. The detector employed a readily available laser pointer as a light source and photodiode IC as a light sensor. The detector was tested using polystyrene latex beads and found to be quite sensitive and reliable.

In order to demonstrate the applicability of the LS detector, it was incorporated into an FI system, which was designed to measure the sulfate concentrations using an approach based on the standard turbidimetric method of barium sulfate precipitation. Reasonable results were obtained considering the

known limitations of this method, which result from variations in the particle size of the precipitate. We believe that this method has considerable promise due to the very reproducible mixing conditions that can be obtained in FI systems. Improvements in the accuracy of the analysis should be possible by optimizing the precipitation conditions to obtain more precise control of the particle size. Work is ongoing in our laboratories to produce a method for sulfate analysis which is more precise and efficient than the commonly used batch turbidimetric procedure.

Acknowledgements

We thank the Thailand Research Fund (TRF) and the Postgraduate Education and Research Program in Chemistry (PERCH) for support. J. J. thanks Thailand-Australia Science and Engineering Assistant Project (TASEAP) for the support of his research at Monash University. Y. U. thanks Thailand Ministry of University Affairs (MUA) for providing his scholarship.

References

1. S. Ross and I. D. Morrison, "*Colloidal Systems and Interfaces*", **1988**, John Wiley, New York, 44 - 47.
2. B. Wittgren and K-G. Wahlund, *Carbohyd. Polym.*, **2000**, *43*, 63.
3. H. H. Stuting and I. S. Krull, *Anal. Chem.*, **1990**, *62*, 2107.
4. R. B. R. Mesquita, S. M. V. Fernandes, and A. O. S. S. Rangel, *J. Environ. Mon.*, **2002**, *4*, 458.
5. B. M. Simonet, F. Grases, and J. G. March, *Fresenius J. Anal. Chem.*, **2001**, *369*, 96.
6. P. J. Worsfold and A. Hughes, *Analyst*, **1984**, *109*, 339.
7. C. O. Costa-Neto, A. V. Pereira, C. Aniceto, and O. Fatibello-Filho, *Talanta*, **1999**, *48*, 659.
8. J. M. Calatayud, S. N. Sarrion, A. S. Sampedro, and C. G. Benito, *Microchem. J.*, **1992**, *45*, 129.
9. J. M. Calatayud and C. M. Pastor, *Anal. Lett.*, **1990**, *23*, 1371.
10. J. M. Calatayud, P. C. Falco, and A. S. Sampedro, *Analyst*, **1987**, *112*, 87.
11. I. P. A. Morais, A. O. S. S. Rangel, and M. R. S. Souto, *J. AOAC Inter.*, **2001**, *84*, 59.
12. V. Kuban, *Fresenius J. Anal. Chem.*, **1993**, *346*, 873.
13. F. J. Krug, E. A. G. Zagatto, B. F. Reis, O. Bahia Filho, A. O. Jacintho, and S. S. Joergensen, *Anal. Chim. Acta*, **1983**, *145*, 179.
14. S. Baban, D. Beetlestone, D. Betteridge, and P. Sweet, *Anal. Chim. Acta*, **1980**, *114*, 319.
15. R. A. S. Lapa, J. L. F. C. Lima, and I. V. O. S. Pinto, *Analusis*, **2000**, *28*, 295.
16. J. F. van Staden and R. E. Taljaard, *Anal. Chim. Acta*, **1996**, *331*, 271.
17. H. Liu and P. K. Dasgupta, *Anal. Chim. Acta*, **1996**, *326*, 13.
18. J. G. Graeme, "*Photodiode Amplifiers*", **1995**, McGraw Hill, 25.
19. Igor Pro, Wavemetrics, Inc., Oregon USA.

Indian Journal of Chemistry
Vol. 42A, December 2003, pp. 2939-2944

Flow injection spectrophotometric determination of As(III) and As(V) using molybdate reagent with solid phase extraction in-valve column

Kate Grudpan[1]*, Ngarmsri Worakijcharoenchai[1,2], Ponlayuth Sooksamiti[3], Jaroon Jakmunee[1] & Gary D Christian[4]

[1]Department of Chemistry, Faculty of Science and Institute of Science and Technology Research and Development, Chiang Mai University, Chiang Mai 50200, Thailand
E-mail: kate@chiangmai.ac.th

[2]Permanent address: Department of Industrial Works, Ministry of Industry, Bangkok 10400, Thailand
[3]Office of the Mineral Resources, Region III (Chiang Mai), Chiang Mai 50200, Thailand
[4]Department of Chemistry, University of Washington, Box 351700, Seattle, WA 98195-1700 USA

Received 10 December 2002

Flow injection (FI) spectrophotometry for speciation of As(III) and As(V) has been investigated. As(III) in a mixture of AsO_2^- and AsO_4^{3-} merging with IO_3^- will convert into As(V). The total AsO_4^{3-} forms heteropoly acids with molybdate reagent. Mo(VI) is subsequently reduced to Mo(V). The compound in the stream flows into an in-valve microcolumn packing with C_{18} resin. The sorbed As-complex is eluted and continuously monitored by an LED colorimeter. The signal corresponds to the sum of AsO_2^- and AsO_4^{3-}. A signal obtained without merging with IO_3^- is that of the AsO_4^{3-} alone in the mixture. Optimization for the conditions has been investigated. Single standard As(V) calibration is possible. Application to a sample free from phosphate such as water leachates of zinc ores has been demonstrated.

Arsenic compounds are used in agriculture as insecticides, herbicides and also in veterinary medicine. Arsenic acid is used as desiccant for the defoliation of cotton boll prior to harvesting and for the preparation of wood preservative salts. Arsanilic acid is used as a feed additive for poultry. Arsenic alloyed with aluminium, gallium or indium forms III-V semiconductors for integrated circuit, diode, infrared detector and laser technology. The toxicity of arsenic depends on its chemical state. Trivalent arsenic compounds (As_2O_3) are usually more toxic to mammalian tissues than the pentavalent compounds (As_2O_5)[1-3]. Various techniques have been proposed for the determination of arsenic, for example, spectrophotometry[4,5], HG-AAS[6,7], ICP-AES[8], ICP-MS[9] and voltammetry[10]. Flow injection (FI) procedures for arsenic determination and arsenic speciation have been reported[11-17]. An FI manifold was reported for sequential determination of AsO_2^- and AsO_4^{3-} for 0.6-18.7 and 1.9-4.75 mg/l respectively. It is based on the reaction of AsO_4^{3-} with ammonium molybdate to form molybdoarsenate which is then reduced to the "molybdenum blue". Oxidation with KIO_3 for conversion of As(III) to As (V) is for the determination of total arsenic[12]. An FI system with a column packed with a resin provides not only on-line preconcentration and separation but also possibility for single standard calibration[18-20]. It also offers speciation such as Fe(II)/Fe(III)[21] and Cr(III)/Cr(VI)[22].

In this work, attempts have been made to develop an FI system comprising simple and low-cost components with C18 solid phase extraction in-valve for preconcentration and separation and for speciation of As(III) and As(V) by sequential determination. AsO_4^{3-} forms heteropoly acids with molybdate reagent. Mo(VI) is subsequently reduced to Mo(V) which is sorbed onto a C18 in-valve column. The sorbed As-complex is eluted and continuously monitored by an LED colorimeter. As(III) in the mixture of AsO_2^- and AsO_4^{3-} is in-line oxidised to As(V), leading to the total As, and As(III) can be obtained by the difference. Optimisation of conditions was investigated. Single standard calibration was studied. Application to water leachate of zinc ores has been demonstrated.

Materials and Methods

All chemicals were analytical reagent grade except where otherwise stated, and de-ionised water was used.

A stock standard As(III) (1000 mg/l) solution was prepared by dissolving $NaAsO_2$ (Carlo Erba) (0.1734 g) in water and diluted to 100.0 ml. A stock standard As(V) (1000 mg/l) solution was prepared similarly from $Na_2HAsO_4.7H_2O$ (BDH) (0.4165 g). Further appropriate dilutions were freshly made. Ammonium molybdate [0.20% (*w/v*)] in sulphuric acid solution (0.25 *M*) was prepared by dissolving $(NH_4)_6Mo_7O_{24}.4H_2O$ (BDH) (2.0 g) in sulphuric acid (0.25 *M*, 1 litre) and kept in a polyethylene bottle to prevent introduction of silica. Ascorbic acid solution [6.0% (*w/v*)] was freshly prepared before use by dissolving ascorbic acid (Roche) (30.0 g) in 500 ml of water and kept in a brown glass bottle. Potassium iodate solution (0.05 *M*) was daily prepared by dissolving KIO_3 (10.7 g) in 1 litre of water.

C18 SPE in-valve column

The laboratory made microcolumn similar to that previously reported[22] was a cylindrical Perspex drilled for 25 mm × 3 mm i.d. The column was filled with the C18 resin (Lichrolut® RP-C18, Merck). The two ends of the column were plugged with porous Teflon frits and covered with fittings for PTFE tubing (0.8 mm i.d.). The column was connected with the injection valve (to replace a sample loop). Connecting of tubing to the valve is designed for reverse flow directions of the standard/sample loading and of the elution to prevent blockage in the column which may be caused by accumulation of the resin at the one end of the column if the loading and elution passed through the column in the same direction[19].

FI manifold

Figure 1 depicts the flow system used. A four channel peristaltic pump (Ismatec, MC-MS/CA 4/6) was used to propel standard/sample solution(s), water/oxidizing agent (KIO_3) (R1) stream, ammonium molybdate in acid solution (R2) and ascorbic acid solution (R3). A three-way valve (Connecta ®, Sweden, normally used for clinical purposes) was used to select the H_2O or R1 stream. RC1 and RC2 were mixing coils for the merged streams of S and H_2O or R1 and the R2 and R3, respectively. The mixing coil RC3 was immersed in a water bath (controlled temperature ±2°C) and connected to the injection valve (V2) (FIAlab-2000, USA), having the in-valve column (C18) as described above. When switching the valve to the loading position, an eluent was pumped by another peristaltic pump (P1) (Eyela, Japan) to elute the sorbed As-complex from the column and pass it through the mixing coil, RC4, before entering into a flow-through cell (Hellma, 1 cm, Suprasil 1 window) in a spectrophotometer (Ismatec, red LED for 820 nm). FIAgrams were recorded by a chart recorder (Philips PM 8521). All connecting tubings were of Teflon (0.8 mm i.d.).

Procedure for sequential determination of As(III) and As(V)

As(V) alone in the mixture was determined first by merging the sample with a water stream controlled by valve V1. The merged stream was further merged with the colouring stream R2. The blue molybdoarsenic acid complex was retained on the C18 microcolumn and eluted by changing the position of the column on the injection valve V2, and the eluted product flowed further through RC4 to the detector (820 nm).

As(III) in the mixture was determined by switching the three way valve, V1, so that the KIO_3 solution (R1) flowed to merge with the sample containing As(V) and As(III). The total As(V) [the original As(V) contained in the sample plus the oxidized As(III)] was merged with ammonium molybdate and ascorbic acid (R2). The sum of As(V) and As(III) was obtained from the signal.

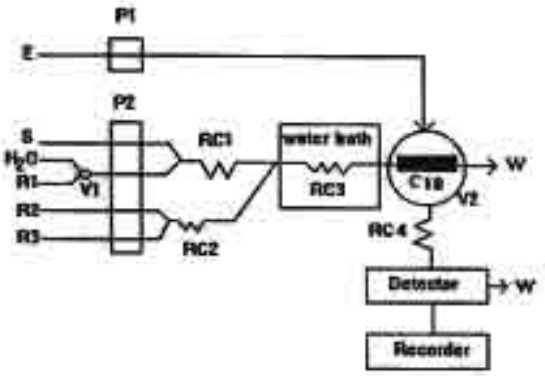

Fig. 1—Flow diagram system for speciation of As(III) and As(V) [P1, P2 = peristaltic pumps, V1 = three-way valve, S = sample, E = eluent, R1 = oxidizing agent (KIO_3), R2 = ammonium molybdate in acid solution, R3 = ascorbic acid, RC = reaction coil, V2 = rotary injection valve, C_{18} = in-valve microcolumn on V2, W = waste].

Results and Discussion

Optimization of the FI manifold

The parameters kept constant were: R1 (KIO_3, 0.05 *M*); R2 [ammonium molybdate (0.10% (*w/v*)] in H_2SO_4 (0.25 *M*); R3 [ascorbic acid [6.0% (*w/v*)]]; RC1 (40 cm); RC2 (80 cm); RC3 (200 cm); RC4 (75 cm); flow rates of R1, R2, R3 and the standard/sample were 1.8 ml/min; eluent (NaOH, 0.10 *M*) with a flow rate of 3.5 ml/min; and a water bath temperature of 55±2°C. The effect of ammonium molybdate concentration in 0.25 *M* H_2SO_4, presented in Fig. 2, indicates that if the concentration of ammonium molybdate was too high the net peak height due to As(V) decreased with increase in the contribution from the blank. An ammonium molybdate concentration of 0.20% (*w/v*) was chosen.

The acid concentration must be controlled. If the acidity is too low, silicate or even molybdate alone will give a blue colour; and if it is too high, the colour due to arsenic is decreased in intensity[20]. A series of calibration graphs [0.10-0.25 mg/l As(V)] was obtained using 0.20, 0.25, 0.30, 0.40 and 0.50 *M* H_2SO_4: y=236x+4.4, y=239x−0.5, y=247x−4.5, y=192x−1.3, y=165x+0.1 with r^2 values of 0.9791, 0.9994, 0.9900, 0.9892, and 0.9946 respectively. The results indicated that maximum slope was obtained in the presence of 0.30 *M* H_2SO_4 but the correlation coefficient was poorer than that obtained in the presence of 0.25 *M* H_2SO_4. A concentration of 0.25 *M* H_2SO_4 was chosen. At this concentration, a linear calibration was obtained passing close to the origin.

When concentrations of ascorbic acid were varied from 2.0-10.0% (*w/v*), an increase in the concentration of ascorbic acid caused an increase in slope of the calibration graph up to a concentration of 6.0% (*w/v*). Increases in concentration above 6.0% (*w/v*) did not alter the slope significantly; therefore for economical reasons, 6.0% (*w/v*) ascorbic acid was selected.

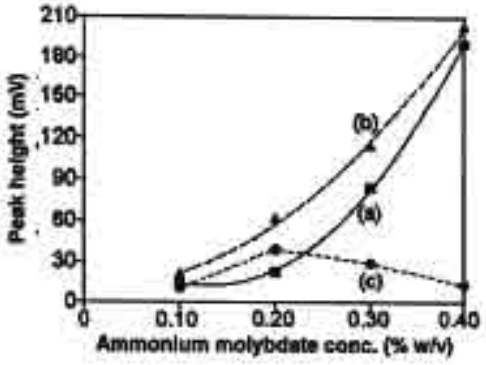

Fig. 2—Effect of ammonium molybdate concentration [(a) blank, (b) 0.25 mg/l As(V) and (c) corrected for blank].

In preliminary studies, various eluents including methanol, ethanol, borax (0.10 *M*) solution (*p*H 9.0) and sodium hydroxide (0.10 *M*) solution, were examined for suitability. The effect of concentration of sodium hydroxide was investigated by varying its concentration between 0.05-0.50 *M* NaOH. It was found that 0.20 *M* sodium hydroxide solution was suitable for further studies.

The effect of eluent flow rate was also studied. It was found that the higher the flow rate, the higher the peak. The flow rate of 4.4 ml/min was chosen as a compromise between peak height and rate of sample injection. This rate is within a region where small variations in flow rate does not alter the peak height significantly.

The effect of flow rate of reagents and sample indicated that peak height increased with increase in flow rate up to a rate of at least 1.8 ml/min. It was noted that above a flow rate of 2.2 ml/min leakage from connections occurred. A flow rate of 1.8 ml/min was therefore chosen.

Peak heights were practically constant for the RC2 (10-80 cm), so 10 cm of RC2 should be used. The optimum RC3 length is 100 cm. The peak height decreased with increase in the RC4 lengths (15-100 cm), so a length of 15 cm should be suitable.

When increasing the KIO_3 concentration, the percent oxidation was increased but peak heights were decreased (Table 1). And if KIO_3 concentration was higher than 0.05 *M*, iodine precipitated in Teflon tubing. An optimum concentration of 0.05 *M* of KIO_3 was chosen.

Table 1—Effect of KIO_3 concentration

KIO_3 conc. (*M*)	Peak height (mV) Blank	Corrected for blank of 0.25 mg/l As(V) (*a*)	Corrected for blank of 0.25 mg/l As(III) (*b*)	Oxidation* (%)
0.025	24	59	26	44
0.05	25	47	39	83
0.06	23	41	34	83
0.07	21	37	32	87
0.08	23	33	28	85
0.10	24	25	25	100

*% oxidation = (*b*/*a*) × 100

The effect of water bath temperature on peak height indicated that peak height increased with increase in temperature up to 55°C. If the temperature exceeded 65°C, air bubbles interfered. Water bath temperature should be maintained at 55°C.

Loading time for As(V) preconcentration

The loading time for 0.01-0.25 mg/l As(V) was varied from 30 to 180 s and with increase in loading time, the slope of the calibration increased. But long loading times decreased the rate of sample throughput. The loading time of 60 s should be appropriate.

The optimum conditions for the sequential determination of As(III)/As(V) are summarized in Table 2.

Analytical characteristics

Using the proposed conditions (Table 2), calibrations were performed as follows: (a) A plot of peak height versus As(V) concentration with the water stream in operation which is used for As(V) determination alone; (b) a plot of peak height with the oxidizing agent stream in operation versus As(V) concentration; and (c) a plot of peak height versus As(III) concentration with the oxidizing agent stream. The three plots were used for evaluation of As(III) and As(V) concentrations in a mixture. From the plots, detection limits (3σ) were estimated[24], as 0.02 mg/l As(V), 0.04 mg/l As(V) and 0.03 mg/l As(III), respectively (a, b, c). Relative standard deviations for As(V) and As(III) were 3.6 and 7.4% [n = 11, 0.1 mg/l for both As(V) and As(III)] respectively (b and c).

Interference study

The effect of interfering ions was studied by loading a blank, 0.10 mg/l As(V) in water stream and 0.10 mg/l As(III) in 0.05 *M* KIO_3 stream in presence of interfering ions. The concentration of an ion is considered to be interfering when peak height lies outside the range $x\pm3\sigma$ where x is the response due to arsenic alone. Results indicate that silicate (as Na_2SiO_3) above 1.0 mg/l, chromium(III) (as $CrCl_3$) and chromium(VI) (as $K_2Cr_2O_7$) above 0.5 mg/l positively interfere. Phosphate seriously interferes due to phosphomolybdenum blue production. Dasgupta *et al.*[25,26] discuss different methods for removal of phosphate and other interferences in similar arsenomolybdate-based measurements.

Table 2—Conditions for the sequential determination of As(III)/As(V)

Reagent R1	0.05 *M* KIO_3
Reagent R2	0.20% (w/v) ammonium molybdate in 0.25 *M* H_2SO_4
Reagent R3	6.0% (w/v) ascorbic acid
Eluent	0.20 *M* NaOH
Flow rate of samples, R1, R2 and R3	1.8 ml/min
Flow rate of eluent	4.4 ml/min
RC1 dimension	80 cm 0.8 mm i.d.
RC2 dimension	10 cm 0.8 mm i.d.
RC3 dimension	100 cm 0.8 mm i.d.
RC4 dimension	15 cm 0.8 mm i.d.
Temperature of water bath	55±2 °C
C_{18} column dimension	2.5 cm 3.0 mm id
Loading time	60 s
LED colour	red
Sensitivity of recorder	200 mV
Chart speed of recorder	0.5 cm/min

Single standard solution calibration for As(V) determination

Standard solutions containing 0.01, 0.05, 0.10, 0.20 and 0.25 mg/l As(V) were loaded at a constant flow rate of 1.7 ml/min through the C18 column, varying the preconcentration times at each concentration. The peak heights of each time were recorded. The results led to five conventional calibrations (a plot of peak height vs μg/ml As), one for each preconcentration time. A plot of μg of As(V) against peak height yields a single line: μg As(V)=flow rate (1.7 ml/min) × [As(V)] (μg/ml) × preconcentration time (min). This indicates that a single standard calibration is linear up to 0.85 μg As ($y=153x+0.74$; $r^2=0.982$).

Analysis of mixtures

The proposed conditions (Table 2) were applied to determine As(III) and As(V) in mixtures. The signals obtained when using a water stream were due to As(V) only; when the oxidizing agent (0.05 *M* KIO_3) stream was used the signals were due to the sum of As(III) and As(V). Percentage recoveries were evaluated. The results are displayed in Table 3. It was found that the recoveries were 96 to 110 and 80 to 100 percent for As(V) and As(III), respectively.

Evaluation of arsenic concentration

Arsenic(V)—As(V) concentration, x_1, can be directly evaluated from the expression:

Table 3—Determination of As(III) and As(V) in mixtures (mean of duplicate injections)

No.	Conc. present (mg/l)		Peak height (mV)		Conc.* found (mg/l)		Recovery (%)	
	As(V)	As(III)	Water stream	Oxidizing stream	As(V)	As(III)	As(V)	As(III)
1	0.10	0	34.0	22.0	0.10	0	100	-
2	0.20	0	64.0	42.0	0.20	0	100	-
3	0	0.08	0	16.0	0	0.08	-	100
4	0	0.15	0	28.0	0	0.15	-	100
5	0.10	0.10	37.0	39.0	0.11	0.08	110	80
6	0.15	0.05	51.0	43.0	0.15_5	0.04	106	80
7	0.04	0.10	12.5	28.0	0.04	0.10	100	100
8	0.25	0	78.0	49.0	0.24	0	96	-
9	0.10	0.08	35.0	37.0	0.10_7	0.07	107	88
10	0	0.25	0	43.0	0	0.24	-	96

*Calculation described in the text.

$y_1 = a_1x_1 + b_1$ ... (i)
or $x_1 = (y_1 - b_1)/a_1$

where y_1 = sample peak height, a_1 = a constant, and b_1 = the peak height of the blank.

Arsenic(III)—The concentrations of As(V), x_2, and As(III), x_3, are evaluated using the oxidizing agent stream from the expressions:

$y_2 = a_2x_2 + b_2$ ... (ii)
$y_3 = a_3x_3 + b_3$ ... (iii)

where y_2 and y_3 are the peak heights of As(V) and As(III), respectively, a_2 and a_3 are constants and b_2 and b_3 are the corresponding blank contributions.

If As(V)=0, $[As(III)]=x_3=(y_3-b_3)/a_3$ ... (iv)

If As(V) ≠ 0 , [As(III)] can be calculated from Eqs (ii) and (iii) as follows:

Peak height due to total As, $h = y_2 + y_3$
$=(a_2x_2+b_2)+(a_3x_3+b_3)$
$=(a_2[As(V)]+b_2)+(a_3[As(III)]+b_3)$
hence, $[As(III)]=\{h-a_2[As(V)]-b_2-b_3\}/a_3$ ... (v)

From the calibrations we obtained:

$y_1 = 315.2(x_1) + 1.141$, $y_2 = 218.2(x_2) + 0.5747$, and $y_3 = 173.4(x_3) + 1.445$

For sample no. 1 in Table 3
As(V) is calculated from $y_1 = 315.2(x_1) + 1.141$

Table 4—Comparative determination of arsenic in ore leaching water samples by proposed method and HG-AAS

Sample No.	As (mg/l)			
	HG-AAS	FIA		
		As(V)	As(III)	Total As
1	0.50± 0.06	0.54	ND*	0.54
2	0.21± 0.02	0.22	ND	0.22
3	2.51± 0.03	2.37	ND	2.37
4	0.75± 0.04	0.84	ND	0.84
5	1.20± 0.03	1.58	ND	1.58

* ND = not-detected

$y_1 = 34.0$ mV hence, $34.0 = 315.2[As(V)] + 1.141$
$[As(V)] = 0.10$ mg/l
For sample no. 3, $y_3 = 16.0$ mV (peak height using water stream = 0)
[As(III)] is calculated from $y_3=173.4[As(III)]+1.445$

hence, $[As(III)] = (16.0-1.445)/173.4=0.08$ mg/l

For sample no. 5, $y_1 = 37.0$ mV
and h (peak height using KIO_3 stream) = 39.0 mV

$[As(V)] = (37.0-1.141)/315.2 = 0.11$ mg/l
$[As(III)]=\{39.0-218.2(0.11)-0.5747-1.445\}/173.4$
$=0.08$ mg/l

Determination of As(III) and As(V) in water samples

The recommended conditions (Table 2) were used to determine As(III) and As(V) in leaching solutions from a zinc ore dump. The results are represented in Table 4. A comparative determination of As(V) by HG-AAS was also carried out. The differences

between the means obtained from the proposed method and the reference method (HG-AAS) were evaluated by a t-test. The calculated t-test value of the proposed-FIA and HG-AAS methods is 0.89. The critical value of t-test is 2.13 (4 degrees of freedom) at the confidence interval of 90%, indicating that the results obtained by the recommended method are comparable to those obtained by the reference method.

Conclusion

A flow injection system with in-valve C18 SPE column for speciation of arsenic(III) and arsenic(V) by sequential determination, based on the formation of a heteropoly acid with molybdate reagent in acid solution and subsequent reduction of Mo(VI) to Mo(V)(molydenum blue), is proposed. As(III) in a mixture of AsO_2^- and AsO_4^{3-} is merged with an oxidizing agent solution(KIO_3) and thereby converted to As(V). The total AsO_4^{3-} is preconcentrated onto a C18 in-valve microcolumn. The sorbed As-complex is eluted and continuously monitored by an LED colorimeter. The signal corresponds to the sum of As(V) and As(III). A signal obtained using water instead of the KIO_3 stream gives the As(V) concentration alone in the mixture.

The method has been applied to a sample free from phosphate, such as water leachates from zinc ores.

Acknowledgement

We thank the Thailand Research Fund and the National Science and Technology Development Agency. The Postgraduate Education and Research Program in Chemistry is acknowledged for partial support.

References

1 Mark H F, *Encyclopedia of chemical technology*, 3rd ed., Vol 3, (Wiley, New York) 1979, pp. 243.
2 *Arsenic in the environment*, Parts I & II, edited by J O Nriagu (Wiley, New York) 1994.
3 Saha J C, Dikshit A K, Bandyopadhyay M & Saha K C, *Crit Rev Envir Sci Technology*, 29 (1999) 281.
4 Johnson D L & Pilson M E Q, *Anal chim Acta*, 58 (1972) 289.
5 Howard A G & Arbab-Zavar M H, *Analyst*, 105 (1980) 338.
6 Maher W A, *Anal chim Acta*, 126 (1981) 157.
7 Yu M Q, Liu G Q & Jin Q, *Talanta*, 30 (1983) 265.
8 Feng Y L & Cao J P, *Anal chim Acta*, 293 (1994) 211.
9 Pozebon D, Dressler V L & Curtius A J, *J Anal At Spectrom*, 3 (1998) 7.
10 Huang H & Dasgupta P K, *Anal chim Acta*, 380 (1999) 27.
11 Hansen E H & Andersen, J E T, *Lab Autom Inform Management*, 34 (1999) 91.
12 Linares P, Luque de Castro M D & Valcarcel M, *Anal Chem*, 58 (1986) 120.
13 Narusawa Y & Hashimoto T, *Chem Letters*, (1987) 1367.
14 Chan C C Y & Sadana R S, *Anal chim Acta*, 270 (1992) 231.
15 Burguera M & Burguera J L, *J Anal At Spectrom*, 8 (1993) 229.
16 Le X C, Cullen W R & Reimer K J, *Anal chim Acta*, 285 (1994) 277.
17 Pozebon D, Dressler V L, Neto J A G & Curtius A J, *Talanta*, 45 (1998) 1167.
18 Grudpan K, Laiwraungrath S L & Sooksamiti P, *Analyst*, 120 (1995) 2107.
19 Sooksamiti P, Geckeis H & Grudpan K, *Analyst*, 121 (1996) 1413.
20 Grudpan K, Jakmunee J & Sooksamiti P, *Lab Robotics and Automation*, 10 (1998) 25.
21 Krokler S, Frenzel W & Schulze G, *Anal Chim Acta*, 296 (1994) 115.
22 Grudpan K, Worakijcharoenchai N, Tue-Ngeun O, Sooksamiti P & Jakmunee J, *Science Asia*, 25 (1999) 99.
23 Sandell E B, *Colorimetric determination of traces of metals*, 3rd ed, (Interscience Publishers, New York), 1965.
24 Miller J C & Miller J N, *Statistics for analytical chemistry*, 3rd ed (Ellis Horwood, Chichester) 1993.
25 Dasgupta P K, Huang H, Zhan G & Cobb G P, *Talanta*, 58 (2002) 153.
26 *Arsenic: Analytical chemistry and beyond*, Special issue edited by P K Dasgupta, *Talanta*, 58 (2002) 1-235.

ผลงานวิจัย ก19